AD-A261 455

OCUMENTATION PAGE

Form Approved
OMB No. 0704-0188

(2)

1)	2. REPORT DATE	3. REPORT TYPE AND DATES COVERED
		ANNUAL 10 Jul 91 TO 09 Jul 92

4. TITLE AND SUBTITLE

THE INITIATION OF LIGHTNING AND THE GROWTH OF ELECTRIC FIELDS IN THUNDERSTORMS

5. FUNDING NUMBERS

F49620-92-J-0020
61102F
2310
CS

6. AUTHOR(S)

Dr John Latham

7. PERFORMING ORGANIZATION NAME(S) AND ADDRESS(ES)

Pure and applied Physics Dept
University of Manchester
Institute of Science ahd Technology
B.O. Box 88
Manchester, UK M60 1QD

8. PERFORMING ORGANIZATION REPORT NUMBER

AFOSR-TR- 93 0046

9. SPONSORING / MONITORING AGENCY NAME(S) AND ADDRESS(ES)

Lt Col James G. Stobie
AFOSR/NL
Building 410
Bolling AFB DC 20332-6448

93-04292

90P9

11. SUPPLEMENTARY NOTES

DTIC
ELECTE
MAR 0 2 1993
S B D

12a. DISTRIBUTION / AVAILABILITY STATEMENT

Approved for public release;
distribution unlimted

12b. DISTRIBUTION CODE

13. ABSTRACT *(Maximum 200 words)*

As specified in the original proposal, there exits mounting evidence that the growth of strong electric fields - culminating in lightning - in the great majority of thunderstorms is intimately linked with - and probably contingent upon - the concomitant development of the ice-phase. Thus, significant progress in the elucidation of electrification mechanisms requires an improved understanding of the complex set of processes involved in cloud glaciation. Accordingly, primary emphasis has been devoted in this first year of a proposed 3-year study, to the analysis and interpretation of data emanating from major airborne experiments in which a primary objective was to seek a superior understanding of the initiation and development in cumulus clouds of the type which ofter become strongly electrified.

14. SUBJECT TERMS

15. NUMBER OF PAGES

16. PRICE CODE

17. SECURITY CLASSIFICATION OF REPORT	18. SECURITY CLASSIFICATION OF THIS PAGE	19. SECURITY CLASSIFICATION OF ABSTRACT	20. LIMITATION OF ABSTRACT
(U)	(U)	(U)	(U)

NSN 7540-01-280-5500

Standard Form 298 (Rev 2-89)
Prescribed by ANSI Std. 239-18

93 3 1 060

THE INITIATION OF LIGHTNING AND THE GROWTH OF ELECTRIC FIELDS IN THUNDERSTORMS

First Annual Report to the U.S. Air Force Office of Scientific Research
Attn. Lt. Col. James G. Stobie

Contract No. F49620-92-J-0020

by

Professor J. Latham
Physics Department
UMIST
P.O. Box 88
Manchester M60 1QD
England

December 1992

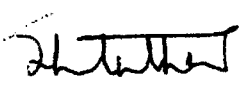

(Professor John Latham)

PREAMBLE

As specified in the original proposal, there exits mounting evidence that the growth of strong electric fields - culminating in lightning - in the great majority of thunderstorms is intimately linked with - and probably contingent upon - the concomitant development of the ice-phase. Thus, significant progress in the elucidation of electrification mechanisms requires an improved understanding of the complex set of processes involved in cloud glaciation. Accordingly, primary emphasis has been devoted in this first year of a proposed 3-year study, to the analysis and interpretation of data emanating from major airborne experiments in which a primary objective was to seek a superior understanding of the initiation and development in cumulus clouds of the type which often become strongly electrified.

As a consequence of the foregoing arguments the kernel of this report, reflecting the primary effort to date, is an extensive account - presented in the form of a paper co-authored by my collaborator Dr. Alan Blyth, and recently submitted for publication in the Quarterly Journal of the Royal Meteorological Society - of this programme of research on thundercloud glaciation.

This primary section is prefaced by a short over-view of the thunderstorm electrification/lightning initiation problem: and is followed by a section which provides a description of laboratory studies designed to extend our knowledge of lightning initiation thresholds in the presence of hydrometers of various types. A paper describing this work was presented at the Ninth International Conference on Atmospheric Electricity, held in St. Petersburg, Russia, in the summers of 1992: and a written version of it - co-authored by my collaborators Dr. Hugh Christian and Dr. Alan Blyth - is reproduced herein.

It is envisaged that the research to be conducted in the second year of this

programme of study will be basically as specified in the original proposal. Primary focus will be placed on:

(1) extension of the glaciation studies described herein,

(2) extension of the laboratory studies described herein,

(3) development of theoretical and computational studies of aspects of the thunderstorm electrification/lightning initiation problem.

THUNDERSTORM ELECTRIFICATION and LIGHTNING : AN OVERVIEW

The development of improved radar techniques and instruments for in-cloud electrical and physical measurements, coupled with a much clearer recognition by the research community that establishment of the mechanism or mechanisms responsible for electric field development in thunderclouds, culminating in lightning, is inextricably linked to the concomitant dynamical and microphysical evolution of the clouds, has led to significant progress over the past decade.

Field studies indicate that in most thunderclouds the electrical development is associated with the process of glaciation, which can occur in a variety of incompletely understood ways. In the absence of ice field-growth is slow, individual hydrometeor charges are low and lightning is produced only rarely. Precipitation - in the solid form, as graupel - also appears to be a necessary ingredient for significant electrification, as does significant convective activity and mixing between the clouds and their environments, via entrainment.

Increasingly, the view is being accepted that charge transfer leading to field-growth is largely a consequence of rebounding collisions between graupel pellets and smaller vapour-grown ice crystals, followed by the separation under gravity of these two types of hydrometeor. These collisions occur predominantly within the temperature range -15 to -30C, and for significant charge transfer need to occur in the presence of supercooled cloud droplets.

The field evidence is inconsistent with an inductive mechanism, and extensive laboratory studies indicate that the principal charging mechanism is non-inductive and associated - in ways yet to be identified - with differences in surface characteristics of the interacting hydrometeors.

Laboratory studies indicate that the two most favoured sites for corona emission leading to the lightning discharge are the tips of ephemeral liquid filaments produced during the glancing collisions of supercooled raindrops; and protuber-

ances on large ice crystals or graupel pellets. The relative importance of these alternatives will depend on the hydrometeor characteristics and the temperature in the regions of strongest fields; which features are themselves dependent on air-mass characteristics and climatological condsiderations.

A recently identified unresolved question is why, in continental Northern Hemisphere thunderclouds at least, the sign of the charge brought to ground by lightning is predominately negative in summer and positive in winter.

Development of Ice and Precipitation in New Mexican Summertime Cumulus Clouds

Alan M. Blyth

Department of Physics and Geophysical Research Center, New Mexico Institute of Mining and Technology, Socorro, NM 87801, U.S.A.

John Latham

Department of Pure and Applied Physics, U.M.I.S.T., Manchester, M60 1QD.

(Submitted to the Quarterly Jornal of the Royal Meteorological Society)

ABSTRACT

An experiment, involving the NCAR King Air, was conducted in order to measure the microphysical properties of New Mexican summertime cumulus clouds. Since the clouds formed and developed essentially in place, over the mountains, it was possible to make multiple penetrations through a single cloud, thereby observing a significant fraction of the cloud's life cycle. In this paper, we address the questions of primary and secondary ice production, and the development of precipitation particles.

Primary ice nucleation was found to occur when the cloud reached a temperature of -10 → -12 °C irrespective of whether this was in the updraught or downdraught. Drops of diameter $D \approx 0.5$ mm, were often observed in concentrations of about 10 L^{-1} prior to the formation of ice which suggests a nucleation mechanism involving large drops. The maximum concentrations of ice particles observed in these clouds (up to about 1300 L^{-1}) are much higher than typical concentrations of ice particles that can be attributed to primary ice nucleation. Evidence suggests that the most likely candidate to explain this enhancement is the Hallett-Mossop process of secondary ice crystal production.

Ice particles were generally first observed in the downdraughts. The development of precipitation is thought to often occur via downdraught transport, followed by sedimentation or mixing of ice particles into fresh, liquid-laden turrets. The multi-thermal nature of the clouds is considered to be central to this process.

1. INTRODUCTION

Traditionally, the production of precipitation inside a cloud is considered in terms of two processes: collision and coalescence of cloud droplets, or accretional growth of ice. They are not necessarily independent. Koenig (1963), for example, found that although the ice phase was ultimately responsible for the development of precipitation in Missouri clouds, the presence of large drops was extremely important in accelerating the process. Braham (1964) summarised many of the results of "Project Whitetop" in Missouri. Some of the important conclusions were: a) the first precipitation particles were predominantly liquid; b) ice was found in clouds whose tops were between -5 and -10 °C as long as liquid drops were present beforehand; c) graupel particles grew at a much faster rate than the liquid counterpart. The nucleation process was thought somehow to be through the freezing of the liquid drops.

Dye et al. (1974) provided a good summary of events prior to NHRE. The results of NHRE, reported by Knight et al. (1974), Cannon et al. (1974), Dye et al. (1974), and Dye et al. (1976) indicated that large liquid drops were scarce in northeastern Colorado cumulus clouds, while ice crystals, aggregates and graupel were in abundance. Also, first echoes from radar were generally well above the freezing level on a consistent basis. Subsequent studies in Montana during HIPLEX by Cooper and Lawson (1984), Hobbs et al. (1980) and others confirmed the conclusions from NHRE about storms in the High Plains of the United States.

There has been renewed interest recently in the role of large liquid drops in the precipitation process, due especially to dual-polarisation radar studies (e.g. Caylor and Illingworth 1987) where small concentrations of such drops can be more readily

detected than with instrumented aircraft. However, large drops continue to be observed in aircraft studies. Dye (1983) found a few liquid drops (photographed by the Cannon particle camera (Cannon 1975)) in amongst the larger number of graupel particles in a New Mexican thunderstorm, although he suggested that they were produced via recirculation. Hobbs and Rangno (1985) associated the production of ice in maritime clouds with the prior existence of liquid drops with diameters, $D > 100\ \mu m$. Blyth and Latham (1990) also found an indication of the presence of liquid drops of diameter $D \approx 100\ \mu m$ in Montanan cumulus studied during the Cooperative Convective Precipitation Experiment (CCOPE) using data from the PMS-1D probe.

Precipitation during New Mexican summers usually falls as rain or small hail from individual thunderstorms. Morning storms are generally limited to mountainous regions, whereas storms that occur at other times of the day seem more inclined to move over the valleys and plains. A large project was conducted recently near Langmuir Laboratory in the Magdalena Mountains, involving four Doppler radars, and three aircraft, to study precipitation development, the electrification, and dynamics of the morning mountain storms. Raymond and Blyth (1989) used particle trajectories calculated using the Doppler radar data to examine the behaviour of precipitation particles in one storm. They concluded that hydrometeors were graupel particles, which formed at the local tops of the precursor clouds to the main storm, and subsequently grew in a manner predicted from a simple model of accretional growth. Based on these analyses, and the direct observations of ice crystals and graupel particles made by Dye (1983) with the NOAA Explorer Sailplane, we believe that precipitation in New Mexican cumulus clouds forms via the ice phase. However, large drops have been observed (Dye 1983) and radar echoes have been known to form initially at

altitudes below the melting level (Dr. Paul Krehbiel, personal communication). So the details of the precipitation process in New Mexican cumulus clouds remain unclear.

It was not possible to determine the origin of the graupel particles using radar data since initial stages of their growth, from the initiation of ice to the beginning of accretion, were missed. The initiation of ice is one of the major outstanding problems in cloud physics.

The problems surrounding the ice phase are of particular interest at this time, because of the need to represent ice processes in global climate models. The processes are complex and thus difficult to parameterise.

The purpose of this paper is to address the questions of ice initiation, and subsequent development into precipitation-sized particles. A secondary goal is to simply describe the microphysical properties of New Mexican clouds.

In Section 2 of this paper, we describe the details of the study and the instruments used to gather the data. The characteristics of the clouds are discussed in Section 3. In Sections 4 and 5, we discuss ice initiation and concentrations of ice respectively, and we consider the development of precipitation in Section 6.

2. DETAILS OF THE STUDY

The summer storms that form over the Magdalena Mountains in New Mexico have been well documented in the literature (Braham et al. 1951; Winn et al. 1978; Raymond and Wilkening 1982, 1985; Dye et al. 1988; Raymond and Blyth 1989, and others). The first clouds form in the morning, often as early as 09:30 local time (MDT: all times hereafter will be reported in MDT). The above studies, and time-lapse photographs, have shown that the cloud systems which develop over the

Langmuir Laboratory typically go through several cycles of growth and decay while the highest tops gradually ascend. It is quite normal for new turrets to ascend through the remnants of their predecessors, in a manner similar to that discussed by Ludlam (1952), Mason and Jonas, (1974), Koenig (1963), and Roesner et al. (1990), for example. This development stage is sometimes followed by a sharp transition to a vigorous thunderstorm as cloud tops rapidly ascend to 12 km or higher, and precipitation and lightning intensity increase dramatically.

One goal of the project was to investigate the development of the cloud particles, from small cloud droplets to graupel pellets. To achieve this end, we used the King Air aeroplane belonging to the National Center for Atmospheric Research (NCAR) during August 1987. It was fully equipped with cloud physics and standard meteorological instruments as well as six field mills to measure the electric field. Multiple penetrations were made approximately every 5 min, chiefly near the tops of several cumulus clouds that formed over the Magdalena Mountains. Since the clouds were always in the same region, it was often possible to observe the development of the clouds from the earliest stages, before ice had formed, through to before the first lightning when the King Air had to leave.

A list of instrumentation typically onboard the NCAR King Air, along with their operating characteristics, is given in Research Aviation Facility (1990). Since we were particularly interested in the characteristics of the particles in the clouds, the aircraft was equipped with a Forward Scattering Spectrometer Probe (FSSP), a 200X 1D probe, and a 2DC (cloud) and 2DP (precipitation) probe (Knollenberg 1970; Knollenberg 1976; Knollenberg 1981; Baumgardner 1986). The size range covered by each instrument, as well as the approximate sample volumes are given in Table 1. The

FSSP has been under considerable scrutiny since its introduction into the field. Processing of FSSP data by NCAR for this project included partial recovery of losses due to coincidences and probe dead time (Baumgardner et al. 1985), and adjustment of channel widths to account for airspeed corrections to the electronics (Cerni 1983; Dye and Baumgardner 1984; Baumgardner 1987). FSSP spectra were not used in great detail in the analysis described herein, and so corrections have not been made for problems in the droplet spectrum due to coincidences, as discussed by Cooper (1988) and Brenguier (1989), or due to laser beam inhomogeneities (Baumgardner and Spowart 1990). Data obtained by the 200X 1D probe were corrected (by NCAR) for time response problems reported by Baumgardner (1987). We performed our own analysis of image data from the 2D probes, although it was modelled after the package used at NCAR. Concentrations were calculated after rejection of zero area images, splashes, streakers, and hollow images. Calculation of the concentration of particles sampled by the 2DC probe was complicated by the frequent omission of the time bar following the timing word. The difficulty was largely alleviated by counting the number of transitions between on and off bits in each word to attempt to distinguish between a particle and a timing word (Dr. Al Cooper, personal communication). The ultimate acceptance of a record depended on comparison between the calculated end time and the beginning time of the next record, and gaps in the plots of 2DC-derived concentrations presented in this paper are due to accumulated elapsed times that sum to a time significantly greater than the beginning time of the next record. The 2DP concentrations were occasionally prone to similar problems.

Analysis of images reported herein relied mainly on visual recognition where possible, with the assistance of simple routines that distinguished between approximately

spherical and non-spherical particles.

Liquid water content was measured by a King probe (King et al. 1978), and a Johnson-Williams probe (Spyers-Duran, 1968). The former saturated at about 1.5 g m^{-3} and was often unusable. The latter has been well discussed in the literature (for example by Strapp and Schemenauer 1982). It is known to have a slow time response which can be as much as several seconds when entering cloud. Values of liquid water content generally compared well with the values derived from the FSSP. However, the FSSP occasionally suffered from serious contamination in the presence of significant ice. The contamination appeared as a flat tail on the spectrum extending out to the largest sizes, giving a liquid water content 3 or 4 times as large as that measured by the Johnson-Williams device. This effect has been described in some detail by Gardiner and Hallett (1985). A combination of JW and FSSP-derived liquid water content was used throughout this analysis. In-cloud temperature was measured at 20 Hz with a platinum resistance thermometer housed in a reverse-flow chamber of the type discussed by Rodi and Spyers-Duran (1972). It had a resolution of about 0.1 °C and a response time of about 0.1 seconds. The aeroplane was equipped with other instruments to measure in-cloud temperature, such as the Ophir radiometer (Lawson and Cooper 1990), but none worked satisfactorily during the project. The reverse-flow probe is known to get wet in warm cloud (Lawson and Cooper 1990), but not in supercooled cloud (Blyth, Cooper and Jensen 1988), and so we limited any detailed analysis involving temperature to supercooled cloud. Dew point was sometimes used to assist in the determination of cloud base, and for this we generally used the EG&G hygrometer mounted on top of the fuselage.

Wind measurements were calculated by NCAR from the inertial navigation system and radome in a manner described by Lenschow and Spyers-Duran (1987). Errors in horizontal winds were experienced during turns, as expected, but our interests were only in straight segments of flight through cloud. Vertical wind is thought to be accurate to within $\pm$ 1 m s^{-1} at best. However, since the results reported herein do not depend critically on the absolute values of any components of the wind, we did not pursue a more detailed investigation of the errors in the air velocities.

An estimation of cloud top was made using the onboard forward-looking video camera. Most penetrations were made within a few hundred metres of cloud top and so the values of cloud top reported herein are probably accurate to within about 200 m. The main source of error is concerned with the horizontal distance from the measuring position to the top of the turret of interest, and this can be exacerbated if the turret has a significant overhang. Such instances are reported as uncertain. The temperature of cloud summit was estimated by extrapolating from the average temperature at the observation level along the saturated adiabat to the altitude of cloud top. This can only be an approximation, and we estimate that cloud top temperatures reported herein are accurate only to within about $\pm$ 2 °C.

We also utilised the Office of Naval Research powered glider (SPTVAR) operated by New Mexico Tech during the project, chiefly to measure electrical properties of the clouds. However, temperature in the lowest levels, and cloud bases were also often derived from SPTVAR measurements. A single in-cloud intercomparison between King Air and SPTVAR was made. The measured temperatures and pressures agreed to within the known accuracies of the sensors.

The aircraft observations were supported on the ground by the Langmuir Laboratory 3 cm radar, observers' notes and photographs, measurements of electric fields, temperature, and amount of precipitation. Radar reflectivities were used to roughly check the cloud top values obtained from the more accurate, but visually limited technique using the on-board video system.

3. CHARACTERISTICS OF THE CLOUDS

General information about the physical properties of the clouds studied by the King Air over the Magdalena Mountains in 1987 is given in Table 2. With many turrets often arising out of the same system of clouds, it is difficult to formulate a clean system of identifying different clouds. In Table 2, we have labelled physically distinct clouds with a different cloud number. Different turrets emanating from the same system are given the same cloud number. Penetrations made through clouds while *en route* to the main cloud of interest are not included in the table. The cloud bases reported were determined either from a single penetration made near cloud base by the King Air, or from when SPTVAR entered cloud near its base. It is quite normal for the bases of these cumulus clouds forming over the Magdalena Mountains to change both with time and space. We would not expect, for example, that the bases of each cloud on the same day be the same as reported in the table, but generally only one measurement of cloud base was made. Thus, the values reported in Table 2 are only approximate (to about ± 2 °C). The cloud base temperatures were in the range 1 °C → 11 °C; about 4.5 → 3.5 km msl. These temperatures are lower by about 20 °C than those of clouds sampled in Missouri by Koenig (1963) for example, and by more than 10 °C than those of Florida cumuli (Hallett et al. 1978). The maximum cloud

tops were determined from the onboard video, and checked with the reflectivities measured by the Langmuir Laboratory radar, as mentioned above. Generally bases were warmer than 5 °C. Therefore, clouds usually spent considerable time without any ice, and many of them were sampled during this period (Clouds 1, 3, 4, 7, 8, 19, and 20).

The altitude of maximum cloud tops varied considerably although it was common for clouds to peak near -15 °C. Those that ascended much above -15 °C developed into vigorous clouds with a greater intensity of precipitation and lightning than those which did not ascend beyond the -15 °C level. Most of the clouds precipitated. The maximum concentrations of cloud droplets did not vary hugely from day to day. Some values shown in the Table are low, but these were obtained either in clouds that already *contained* substantial amounts of ice in the first penetration, or in detrained regions of cloud. This is quite different from cumulus clouds in Montana where maximum concentrations could vary by factors of 2 (e.g. Blyth and Latham 1990). Cumulus clouds in the New Mexico summer only form when there is an intrusion of moist air from the south. Therefore it is likely that the air mass will have similar properties from day to day, with approximate constancy of N, as observed. The cloud droplet spectra were quite broad considering the number of drops, as shown in Figure 1 which presents typical spectra sampled at three altitudes above cloud base. There were significant numbers of large cloud drops with diameter $d > 25\ \mu$m in almost all penetrations. The spectra sampled in the upper two levels of cloud extend from the smallest detectable sizes to $d \approx 50\ \mu$m. These are broader than typical spectra observed in the High Plains storms of the US (e.g. Blyth and Latham 1990), but similar to those measured in Florida by Keller and Sax (1981), and also in Missouri by

Koenig (1963). The 10 Hz spectra at upper levels were also frequently bimodal, consistent with the findings of Warner (1969).

Figure 2a presents the details of the 20 Hz vertical wind observed in Cloud 3 (9 August). The pattern of a near-zero penetration average with a wide range of values between -10 to +10 m s^{-1} is typical of all the clouds. Values of 100 m averaged vertical wind for *all* the cumulus clouds studied in the project are illustrated in Figure 2b. Stronger updraughts may have been missed since it was not possible, for safety reasons, for the King Air to penetrate regions of cloud that had reflectivities of 30 dBZ or more, measured by the onboard radar. The results shown in Figures 2a & b are consistent with the observations discussed by Raymond et al. (1991) who used Doppler radar data from the project in 1984 to determine vertical and horizontal mass fluxes. They found that the updraughts and downdraughts were of comparable magnitude in the early stages of New Mexican cumulus clouds. Figure 2b also indicates that it was uncommon to observe updraughts or downdraughts with a magnitude, averaged over 100 m, of greater than 5 m s^{-1}.

Very little positive buoyancy was observed in these clouds despite the presence of significant updraughts. Indeed, many of the cloudy regions sampled were close to being neutrally buoyant. Also, undiluted regions of cloud were rarely encountered. This general lack of positive buoyancy in 10 m s^{-1} updraughts, and scarcity of adiabatic parcels, was probably a consequence of the tendency to penetrate the clouds very close to their summits. The one cloud in which undiluted cloud regions were frequently measured (Cloud 23) was sampled at least 1 km below cloud top, and it was also a particularly vigorous cloud.

4. INITIATION OF ICE

Despite the inevitable speculation that arises from measurements conducted in a such a large spatial and temporal domain, we have obtained clues to the processes involved which point to the conclusion that ice first forms, in these New Mexican clouds, at a temperature near -12 °C. We illustrate the results that led us to this conclusion in the following paragraphs.

Many of the clouds were free of ice for some portion of their lifetime. Ice was observed to form during the course of these studies: Table 3 gives details of when ice particles were first detected by the 2DC probe in these cases. Spherical particles were detected, in some cases, before the times reported in the table. These may be frozen, but we take as the time of first ice to be when particles detected by the 2DC were recognizable as ice. The conclusions reached below are not altered by this uncertainty. The summit of all the clouds reported in Table 3 was colder than -11 °C in all cases, with the exception of Cloud 2 where the summit temperature was estimated to be about -10 °C. Also, cloud tops were never colder than about -15 °C. It is reasonable to assume from this, and the known temperature dependence of nucleation mechanisms, that the formation of ice occurred when the cloud ascended to a sufficiently cold temperature.

As noted in Table 3, large drops (liquid or solid; diameter, $D \approx 500\,\mu m$) were detected by the 2DC probe prior to the formation of non-spherical ice particles in Clouds 2, 3 and 4. The Langmuir Laooratory radar measured low-level echoes that extended no higher than about 6 km msl in these clouds. They were probably a consequence of large drops. Similar echoes were also detected in the early stages of Cloud

1, and in a few other clouds that were not sampled by the King Air. Particles were detected by the 1D probe in Cloud 1 before the times noted in the table while cloud top was warmer than 0 °C, and also in updraught regions with $T < 0$ °C of Cloud 8. A few indistinguishable particles were detected sporadically in Cloud 20 for some 30 minutes or so prior to the time given in Table 3, when larger numbers of ice particles began to be observed in the developing turrets. Radar echoes were also observed at an earlier time, but they were from different turrets several kilometers distant from the ones being studied by the King Air.

In all but Cloud 8, the first ice particles were observed in turbulent air, or in the downdraughts, and were markedly absent from the updraughts. For example, the penetration shown for Cloud 3 (9 August) in Figure 3, was made at a temperature of about -7 °C, while cloud top was considerably higher at about -15 °C (see also Table 3). Notice that the updraught is almost void of particles while the downdraught region, encountered on entry into cloud, contained particles in concentration up to about 20 L^{-1}. Some of these particles may in fact be water drops since the 2D images are difficult to identify, although ice particles can clearly be distinguished.

The very first ice particles were missed in Clouds 4 and 8, since graupel were among the first particles to be detected. A radar echo of about 30 dBZ extending up to 7 km msl ($T \approx$ -15 °C) developed from the low-level echo measured in Cloud 4 mentioned above. The development was missed probably because the aircraft was near the base of the cloud when cloud top was approaching the critical temperature for the formation of ice. Cloud 8 was out of the range of the radar. However, cloud top was about 1 km above the aircraft for the two penetrations prior to the first detection of ice. Graupel most likely developed in the upper regions of the cloud during

this time, and subsequently descended to the observation level.

Generally the first ice particles were small ($D \approx 100$ μm) lightly rimed or unrimed, and had indistinguishable habits. However, as already mentioned, graupel of diameter $D \approx$ 1-2 mm was among the first ice particles detected in Clouds 4 and 8.

We illustrate the first-ice results in a different manner in Figures 4 a-f, which show the flux of particles of diameter $D < 500$ μm detected by the 2DC, plotted against the normalised distance across the cloud, with upshear side on the left when penetrations were made parallel to the wind (Figures 4a, & d-f). Cloud 2 is not included in these figures because the ice particles were in a turbulent detrainment region of cloud, rather than associated with the cloud turrets. The flux is downward everywhere except in Cloud 8 (Fig. 4e), where there are similar upward and downward fluxes. These figures clearly illustrate that the first ice was generally observed in the downdraughts. They also indicate that, at least in some cases, there was a larger flux of ice on the downshear side.

Maximum cloud tops remained near -15 °C for the duration of the study on 19 August (Cloud 9), and all penetrations were made within 500 m of cloud top. It was common on this day to find updraughts that contained either considerably fewer ice particles than the downdraughts, or else sections of the updraughts with no detectable ice particles. Figure 5 illustrates an example of the former. The temperature of the penetration was $T \approx$ -13 °C, and cloud top was about 400 m above, with $T_{ct} \approx$ -15.5 °C. There was only a small number of particles in the central updraught region, while the downdraughts, and part of the updraught contained up to about 10 L^{-1} of particles detected by the 2DC. The downdraughts mostly contained lightly rimed or pristine

particles with an average size of $\overline{D} \approx 400$ μm, but with a maximum diameter of nearly 800 μm. Many of the pristine ice crystals were stellar, indicative of growth near -13 °C. Graupel was also present during this pass, particularly in the first part of the updraught. Some of it was larger than 3 mm.

These results are consistent with those of Dye et al. (1976), Heymsfield et al. (1979), and Dye et al. (1986a; 1986b), all of whom observed ice to be present in the downdraughts of cumulus clouds.

It is possible that ice was first observed in the downdraughts because they, or the region in the vicinity of the cloud summit, are where cloud droplets are likely to be evaporating. Young (1974), and Hobbs and Rangno (1985) suggested that contact nucleation may be responsible for the initial formation of ice; Young showed that the probability of a nucleus coming into contact with a cloud droplet is enhanced due to phoretic forces if evaporation is occurring. However, Baker (1991) has demonstrated that phoretic effects are unlikely to cause ice nuclei to be forced into contact with supercooled cloud drops in cumulus clouds since the fluxes caused by temperature and water vapour gradients are significant over too small a distance. The results from the New Mexican cumulus clouds somewhat corroborate this conclusion since the conditions conducive to phoretic transport - evaporation of drops causing a net flux of nuclei towards the cloud drops - are present at all levels in the cloud, and contact nucleation is thought to become effective at a warmer temperature than the temperature of nucleation, $-10 \rightarrow -12$ °C, found herein (Gokhale and Goold 1968).

Other ice nucleation mechanisms may be linked to the evaporation of cloud droplets. For example, Rosinski and Morgan (1991) found enhanced nucleation when

cloud droplets began to evaporate. In order to test if ice crystals were *only* nucleated near cloud top, or in the downdraughts, we used the results of Ryan et al. (1976) for the growth rate of ice crystals at various temperatures in a water saturated environment, to estimate the time taken for pristine ice crystals to grow to the average diameter, $\overline{D}$ = 400 μm observed in the cloudy downdraughts of Cloud 9 on 19 August (see Fig. 5). Growth rates at between -13 and -15 °C are large; $dD/dt \approx 1.2$ μm s^{-1}. Using an average vertical wind speed of $\overline{w}$ = -2 m s^{-1} a particle that had formed in the downdraught, or at the then current cloud top, would have had to be transported downwards a distance of about 600 m in order to grow, by diffusion, to the average size, and more than 1 km for the particle to grow to the larger sizes observed (800 μm). Cloud top was *at most* 400 m above, so it is possible to explain how the particles would form in the downdraught, or at cloud top ($T_{ct} \approx$ -15 °C) and grow to the observed average size (400 μm) if the downdraught was weaker than -2 m s^{-1} at higher levels, but it is difficult to explain the larger sizes. Similar calculations were performed for the few other cases where pristine crystals could be identified in the downdraughts. All the results suggest that, at least for the average size and larger particles, diffusional growth would have had to start in the updraught at about -12 °C, or warmer, and continue as the particles first ascended in the updraught, and then descended to the point of observation in the downdraughts. In other words nucleation commenced, in these clouds, in the updraught at about -12 °C.

The results suggest that neither cloud top, nor the downdraughts are of particular importance for the initial nucleation of ice. However, it *is* clear that downdraughts are important for the redistribution of ice to warmer temperatures, as evinced by results in Figure 4, for example. We shall return to this topic in Section 6. It is also true that

the critical nucleation temperature will be reached first in the ascending cloud top region, or in cooler downdraughts, and this is presumably important to clouds that do not ascend much above the -10 °C level. Furthermore, the smaller particles observed in the downdraughts in the above analysis probably were nucleated in the downdraughts or near cloud top. Their presence may be attributed to a nucleation mechanism associated with the evaporation of cloud droplets, as suggested by the observations of Rosinski and Morgan (1991). Whether or not the concentration of ice particles is greater in downdraughts than concentrations of ice nuclei, or than the concentrations in the updraughts remains to be investigated.

Large drops are thought to play a crucial role in the formation of ice in the maritime cumulus clouds discussed by Hobbs and Rangno (1985). Large drops were directly observed in several of the cases discussed herein before the formation of ice and their presence can be inferred from low-level radar echoes in several others. Thus, it is quite likely that they play a role in primary ice nucleation in New Mexican cumulus clouds as well. Other capture processes, such as inertial scavenging, have a greater effect for larger drops, so it is possible that contact nucleation is important when these drops are present (Baker 1991).

Updraughts void of any type of particles other than those detected by the FSSP were observed in a few cases at -15 °C. The observation is seemingly in contradiction to the notion that ice crystals are nucleated at about -12 °C some 500 m below. However, particles are likely to be too small to detect with the 1D, or 2D probes if they grew by diffusion at about 1 - 1.5 $\mu m\ s^{-1}$ in an updraught of greater than about 5 $m\ s^{-1}$. The measurements gathered in one penetration through Cloud 14 lend support to this argument. Small particles (average diameter, $\overline{D} \approx 100\ \mu m$) were present in the

weaker part of an updraught at -15 °C. Using the average updraught speed of 3 m s^{-1} measured at the observation level, the particles could be traced back to a temperature, $T \approx$ -12 °C. Figure 6 presents data from this penetration showing that particles are smaller in the stronger part of the updraught, and that the maximum size steadily increases into the downdraught. The largest particles are absent from the updraught. Examples of small ice crystals in updraughts were found in other cases, but the trend revealed in Figure 6 was never as clear. Nevertheless, the size of these crystals was always consistent with nucleation at a temperature of approximately -12 °C. It is likely that if nucleation occurred at a higher temperature of -5 °C for example, particles would have rimed by the time -15 °C was reached. Rimed particles were found in several updraughts, but, possibly more importantly, they were noticeably absent from a significant number. Their *presence* can be readily explained in terms of sedimentation, for example, as discussed in Section 6.

Ice developed in three clouds whose tops did not ascend above about -12 °C (Clouds 2, 4 & 5; see Table 2). For example, the summit of Cloud 5 (11 August) measured by the onboard video camera was only slightly above the observation level ($T_{ct} \approx$ -12 °C). Reflectivities from the Langmuir radar confirmed this value and furthermore showed that the cloud (detectable by radar) did not reach a higher altitude before the beginning of the aircraft study. Small irregular ice particles with $\overline{D} \approx$ 80 μm were observed in the downdraughts encountered in the penetrations made near cloud top. These sizes are consistent with the notion that the particles were nucleated near -12 °C (which is cloud top in this case) and were carried down to the observation level in the downdraughts. Similar results were found in the other two cases.

The arguments presented above can be summarised as follows:

- ice particles were first detected when cloud top reached a temperature colder than about -10 °C;
- the first ice particles were generally observed in the downdraughts;
- unrimed ice crystals were observed in downdraughts with sizes that are too large for the crystals to have grown solely in the descent from cloud top;
- small ice particles were observed in the updraughts with sizes indicating an origin of about -12 °C;
- ice particles were observed in clouds whose tops never become colder than about -12 °C.

The evidence suggests that ice nucleation occurs in these New Mexican cumulus clouds at a temperature of about -10 → -12 °C, and that the downdraughts, while important for transporting ice particles to warmer regions of cloud, and perhaps for introducing more ice nuclei, as suggested by Heymsfield et al. (1979), do not necessarily provide a unique environment for contact, or any other nucleation mechanism.

We have made several assumptions in arriving at the above conclusions. Some of these are not directly testable due to the nature of the sampling techniques available to us. Of particular concern is the lack of information about the variability of the vertical wind speed with time and space. The conclusion that ice forms in the updraught at about -12 °C would not be correct if *all* pristine particles in the downdraught were too small to have originated from -12 °C in the updraught. This situation was not observed. However, only a few cases could be used in the analysis since pristine ice crystals were not observed in many situations, probably because of the relatively high

riming rate that occurs if L is significant (e.g Cooper and Lawson 1984), and also because of image recognition problems when small particles have habits other than stellar (Brown 1989). Thus, we draw our conclusions about the trajectories of ice crystals growing by diffusion with some diffidence, noting the need for further studies.

5. CONCENTRATION OF ICE PARTICLES

Figure 7 illustrates concentrations of first ice particles plotted against both the temperature at cloud top and the observation level. All the values deviate from the dashed line shown in the figure - the approximate numbe. of particles that would be activated by primary nucleation if ice nuclei were present in concentrations predicted by the relationship of Fletcher (1962). A number of studies have shown that there is fair agreement between the number of ice crystals that have formed from primary nucleation and the numbers of ice nuclei (e.g. Mossop et al. 1972; Jayaweera and Ohtake 1973; Gagin 1975; Heymsfield et al. 1979; Cooper and Saunders 1980; Cooper and Vali 1981; Rogers 1982). Mossop (1985a) and Cooper (1986) discuss these in more detail. Of particular note is the study by Heymsfield et al. (1979) who found similar concentrations of ice particles and ice nuclei in undiluted updraughts. Figure 7 also shows the geometric-mean of concentrations of ice particles that could be attributed to primary nucleation (Cooper 1986). They are larger than, but within an order of magnitude of the Fletcher curve. The three lower concentrations of first ice in the New Mexican clouds are similar to the results summarised by Cooper, suggesting that, at least in the 3 cases, the first ice is produced by primary nucleation. Ice nuclei were not measured in this project and so this can only be a suggestion. The largest concentrations shown in Figure 7 may contain a contribution from water drops which were

indistinguishable from ice.

The cloud maximum concentration of ice particles for all of the cumulus clouds studied during the project are plotted versus temperature in Figure 8. Both the temperature at the penetration altitude and the temperature of the maximum cloud top up to when the maximum concentration was measured is given in the figure. Observations in these New Mexican clouds do not appear to be consistent with the idea that ice particles are produced by the passage of the aircraft through supercooled cloud (Rangno and Hobbs 1983). Specifically, the concentrations shown in Figure 7 are close to those of ice particles produced by primary nucleation (Mossop 1985a; Cooper 1986). Ice only formed, in these clouds, when cloud top reached about -10 → -12 °C; and localised large concentrations of ice particles with similar shapes were not detected anywhere within these clouds. Thus we have not limited the data presented in Figure 8 to data from the first penetration by the aircraft.

In most of the cases, the maximum concentration of ice particles observed were probably lower than actual values in the clouds for several reasons. Firstly, in several cases the aircraft had to leave the study not long after ice had first formed in the cloud because of fuel considerations. Secondly, it is unlikely that the small region of cloud sampled by the 2DC contained the largest concentrations, particularly when the most intense part of the storm was avoided to minimise the risks of aircraft damage. Also, it is important to emphasise that the concentrations reported are only those derived from the 2DC probe: maximum concentrations which included smaller sizes of ice particles would presumably be much greater.

As Table 2 indicates, the maximum concentration of particles measured by the

2DC was about 1300 L^{-1} in Cloud 15. The temperature of cloud top at the time was $T_{ct} \approx$ -20 °C and the temperature at the observation level was $T \approx$ -17 °C. Concentrations of ice particles larger than 100 L^{-1} were measured in eight clouds.

Ice concentrations were notably lower in several clouds (Clouds 1, 3, 5, 9, 11, 12, 13, 17, and 20). In four of these cases (Clouds 5, 11, 13 and 17) ice formed as the cloud began to decay, so the aircraft left for a more promising cloud. Fuel was short in two other cases (Clouds 1 and 3), so the study ended just as ice formed. A vertical descent was made to lower, warmer levels of Cloud 12, and the 2DC probe failed during study of the last cloud in the project (Cloud 20).

The one cloud studied on 19 August (Cloud 9) is an important exception. Turrets often ascended to -16 °C, and subsequently descended to a general level near -13 °C. The aircraft did not intentionally avoid any regions of cloud, and the cloud did not collapse at any time during the hour-long study. Yet the maximum concentration of ice particles measured by the 2DC probe was only about 40 L^{-1}. The value is still larger than typical values described by Mossop (1985a) and Cooper (1986), but is considerably smaller than the concentrations found in many of the New Mexican clouds. For example, concentrations of about 255 L^{-1} and 700 L^{-1} were measured in Clouds 6 and 18 respectively, which had similar cloud tops.

The number of ice crystals observed in New Mexican clouds was often much greater than expected from primary nucleation (dashed line in Figure 8). This is a familiar result which has provided a dilemma for cloud physicists for many years. There have been many reports of ice particle concentrations that are much higher than typical concentrations of ice nuclei (e.g. Mossop 1968; Mossop and Ono 1969;

Mossop et al. 1972; Hobbs and Atkinson 1976; Hallett et al. 1978; Mossop 1985a; Mossop 1985b; Hobbs and Rangno 1985; Harris-Hobbs and Cooper 1987; Gamache 1990; Rangno and Hobbs 1991).

It is possible that there are more ice nuclei active at a particular temperature than the Fletcher curve predicts. The measurement of ice nuclei is a difficult one and current methods may not represent the conditions in the atmosphere, mainly because only one mode of nucleation (usually deposition) is used. However, as discussed above, measurements of ice concentrations that could be attributable to primary nucleation have indicated that concentrations of ice nuclei and ice particles agreed to within an order of magnitude (see Heymsfield et al. 1979; Mossop 1985a; and Cooper 1986). Ice nuclei were not measured in the present study, but it is unlikely that the concentrations of more than 100 L^{-1} with cloud tops at -15 °C, found in the present study are a result of primary nucleation.

A number of secondary ice crystal production processes have been suggested to try and explain the above dilemma; we refer the reader to Pruppacher and Klett (1980), Mossop (1985a), and Dong and Hallett (1989) for summaries of these processes. Among them, the Hallett-Mossop process has received the most attention. Experiments, reported by Hallett and Mossop (1974) and Mossop and Hallett (1974), showed that splinters were produced during riming, when the temperature was in the range -3 → 8 °C. These, and subsequent experiments (e.g. Mossop 1976) have shown that the process requires both small ($d \leq 13$ μm) and large ($d \geq 24$ μm) cloud drops to coexist with graupel particles. As discussed by Dong and Hallett (1989) the physical mechanism responsible for the production of the splinters is still a matter of some concern. So direct verification of the operation of the Hallett-Mossop process in

clouds is difficult. However, several studies have presented supporting evidence despite the difficulties (e.g. Mossop 1970; Mossop et al. 1972; Hallett et al. 1978; Keller and Sax 1981; Harris-Hobbs and Cooper 1987). The reader is referred to Mossop (1985a) for a summary of results prior to 1985.

We found the most likely explanation for the large concentrations of ice particles to be the Hallett-Mossop process of secondary ice crystal production. This conclusion is based upon several pieces of evidence, which we now describe.

- There were many more ice particles than suggested by estimates of primary nucleation; see Figure 8.

- The maximum concentration of ice particles (shown in Figure 8 plotted against temperature) exhibits only a slight dependence on temperature. There should be a much stronger dependence if the production of ice was dominated by a primary nucleation process (Mossop 1985a; Hobbs and Rangno 1985; Cooper 1986; Harris-Hobbs and Cooper 1987).

- The cloud droplet spectra in most of the clouds were broad with many tens of drops per cubic centimetre of diameter, $d \geq 24$ μm and with $d \leq 13$ μm; see Figure 1, for example.

- Graupel particles were often observed in cloud in the correct temperature range. Even in cases where graupel was not actually observed in this region, their presence can be inferred since rimed particles were frequently observed at higher altitudes.

- The number of droplets of size $d \geq 24$ μm in cloud between -3 and -8 °C was considerably lower than on other days in the one case (Cloud 9, 19 August) where the concentration of ice particles was unusually low, despite cloud top being colder than -15 °C for more than 1 hour. This is illustrated in Figure 9. The cloud drop spectrum measured in Cloud 9 was considerably narrower than those measured in other clouds most likely because cloud base was higher than normal on this day (see Table 2). Moisture was in the process of returning to the state of New Mexico after a prolonged dry spell, and the environment was still quite dry.

Mossop (1978) suggested that the number of splinters ejected in the Hallett-Mossop process depends on the ratio of small ($d \leq 13$ μm) to large ($d \geq 24$ μm) cloud droplets accreted by graupel particles, the cloud temperature, the terminal velocity, and concentration of the graupel particles. There are many uncertainties associated with a simple calculation of how many ice particles are to be expected within a certain time; it is impossible to know how many particles are really involved in the process, and what the trajectories of the resulting splinters would be. Also, the number of small and large drops, and the number of graupel particles are highly variable both in space and time. Even if these were well known, the rate at which splinters are produced by the Hallett-Mossop process remains uncertain (Chisnell and Latham 1976; Mossop 1985b; Mossop 1985c; and Beheng 1987). Harris-Hobbs and Cooper (1987) performed detailed analysis on a number of clouds in three different locations in the U.S. and found good evidence that the Hallett-Mossop process was responsible for the observed concentrations of ice crystals. They found the strongest dependence on the number of graupel particles present, but they also found a dependence on the number

of small and large drops.

Hobbs and Rangno (1985) and Rangno and Hobbs (1991) found that the largest concentrations of ice particles occurred in clouds that previously had the broadest cloud droplet spectrum, which is indicative of the Hallett-Mossop process. However, Rangno and Hobbs (1991) calculated that large concentrations of ice particles were produced far too rapidly to be explained by this process. They proposed instead, on the basis of their observations and on the laboratory work of Blumstein et al. (1987) and others, that rapid nucleation could occur if there were regions within the cloud of enhanced supersaturations with respect to water. The rates at which numbers increased in the New Mexican clouds are lower than the rates discussed by Rangno and Hobbs. The most rapid increase in particle numbers was 10 to 700 L^{-1} in about 20 minutes which is slower than the increase by factors of 100-1000 in 10 minutes observed by Rangno and Hobbs.

It is not at all clear that the Hallett-Mossop process is responsible for the entire development of New Mexican thunderstorms. If it is, the large concentrations of ice particles observed at temperatures of -15 °C or colder (see Table 2) must be accounted for by a process that operates several kilometres below. Keller and Sax (1981) associated the large concentration of ice particles (over 900 L^{-1}) measured at -13 °C in Florida cumuli with splinters produced by the Hallett-Mossop process at lower levels. They emphasised the importance of the multiple thermal mechanism, that also operates in New Mexico clouds, in providing the required particles for the Hallett-Mossop process to operate and for the upward transport of the splinters. Figure 10 demonstrates that there was a significant upward flux of ice in some New Mexican clouds. The figure presents the flux of particles of size $D < 500\ \mu m$, calculated for

six individual turrets which had both ice particles and a significant updraught, plotted against normalised distance in a downwind direction across the cloud. Of course, we cannot associate the ice contributing to the flux as being associated with any particular process. The figure also shows that at least some of the turrets have the classical thermal-like structure with downdraughts flanking the updraughts, and with a tendency for a slightly larger flux on the downwind side. A similar pattern of downdraught distribution was reported by Blyth, Cooper and Jensen (1988) for cumulus clouds in Montana.

Other multiplication processes, such as the raindrop freezing and splintering process treated by Hobbs and Alkezweeny (1968) and Chisnell and Latham (1976), could also have contributed to the high concentrations of ice particles. Raindrops were not observed once ice had formed so it is unlikely that this process dominated ice multiplication. It cannot be ruled out, however; the absence of large drops may be a consequence of probe sample volumes and flight pattern limitations.

6. DEVELOPMENT OF PRECIPITATION

It is clear from this study, and from Dye (1983) and Raymond and Blyth (1989) that precipitation particles in New Mexican cumulus clouds are primarily graupel. In this section, we investigate the development of precipitation by considering the behaviour, and distribution of graupel particles, and of particles that form the graupel embryos. Similar, but more extensive studies of the precipitation process were made during the National Hail Research Experiment (NHRE), the results of which are discussed by Knight et al. (1974), Cannon et al. (1974), Dye et al. (1974), and Dye et al. (1976).

Figure 11a shows the concentration of particles in 1 second samples of cloud (about 100 m) in all updraughts and downdraughts of strengths $|w| > 3$ m s^{-1}, plotted against temperature. For those samples taken from the updraught, all cloud regions with $T \geq -13$ °C have been included, while only those samples with $\overline{D} > 500$ μm are included if $T < -13$ °C. We have argued above that new particles in updraughts at -15 °C, for example, should be much smaller than 500 μm if nucleation does not occur until about -12 °C. Particles nucleated at about -12 °C would be too small to be detected by the 2DC, hence the inclusion of all particles if $T \geq -13$ °C. Thus, at least some of the particles found in updraughts, i.e. roughly those indicated by squares in Figure 11a, must have been introduced into the updraughts either by mixing, or by sedimentation. It is likely that once embodied therein the particles are able to grow quite rapidly by accretion.

Figure 11b is a similar plot showing the number of particles in more quiescent cloud, with $-3 \leq w \leq 3$ m s^{-1}. There are many more regions of cloud falling into this category (also see Figure 2b). Indeed, there are relatively few 100 m regions of cloud with $w > 3$ m s^{-1} irrespective of whether or not they contain ice. Also, the number of particles in these quiescent regions of cloud often far exceed the numbers in the updraughts or downdraughts. The highest concentrations of ice particles were found in regions of cloud with low liquid water content, and small vertical winds ($|w| < 3$ m s^{-1}). This lends support to visual observations, and results of more specific analysis of individual clouds which shows that a considerable fraction of the ice particles are transported away from the main turret activity into an anvil or detrainment layer.

The updraughts were generally among the regions that contained the lowest con-

centrations of ice particles, although the concentration was greater than 100 L^{-1} in at least a few upward moving cloud regions. As expected it is the updraughts that generally had the highest liquid water contents, although there were a few exceptions. Occasionally, very little liquid was observed in updraughts with $w > 3$ m s^{-1}, that also contained large concentrations of rimed ice and graupel particles. Presumably the liquid was depleted due to accretion. A similar observation was made by Heymsfield et al. (1979).

Figures 12a and b show the concentration of particles, with $D \geq 3$ mm detected by the 2DP, plotted against L/L_A for similar conditions as in Figures 11a and b. By far the largest concentrations of these particles were observed in regions of very low liquid water content, and light vertical winds (Fig. 12b). Further examination shows that these particles are large aggregates. On the other hand, the updraughts (with $w >$ 3 m s^{-1}) containing large particles generally have values of $L/L_A > 0.5$. This is hardly a surprising result.

There seems therefore, to be two general fates of ice particles: to encounter liquid water and grow as a graupel particle, or to be carried away from the main turret activity. A change of fate may arise due to the arrival of one of the several fresh turrets that ascend through older cloud, or, similarly, due to the cessation of an updraught. These fates have been more thoroughly investigated with particle trajectories calculated using Doppler radar data described by Miller et al. (1988), Raymond and Blyth (1989), and others.

The particle selection processes suggested by the patterns shown in Figures 12a and b are illustrated in more detail in Figure 13 for a single penetration through Cloud

14 (22 August). The majority of the penetration was made through a detrainment layer where the concentration of ice particles was quite high, and the liquid water content, and vertical wind was low. Particles in this region were pristine, or lightly rimed. In contrast, a turret was encountered towards the end of the penetration, with $w_{max} \approx 7$ m s^{-1}, $L_{max} \approx 1.5$ g m^{-3}, and containing less than 0.5 L^{-1} of relatively large graupel particles ($\overline{D} \approx 2$ mm). Clearly growth was favoured in the liquid-laden turret.

During this penetration the largest graupel particles were found in regions of cloud which contained the lowest concentration of ice particles. Particles were smaller when larger numbers were present. The result is generally the same when all cumulus clouds in the project are considered, as Figure 14 illustrates. The figure shows the concentration of particles detected by the 2DC versus the maximum size of particles detected by the 2DP in 10 m of cloud, for all cumulus clouds studied in the project. We have limited the values to those in cloud with $L > 0.1$ g m^{-3} to avoid including large aggregates. It should be noted that the number of samples containing large graupel particles ($D > 2$ mm) was small, mainly because the aircraft avoided regions of cloud which produced a reflectivity of 30 dBZ, or greater on the on-board radar. Also, although the same conclusions can be made when 1D probe concentrations are used instead of those from the 2DC, small ice particles may nevertheless have been missed in regions of larger graupel particles. It was difficult to eliminate all artifacts and they are likely to be the cause of the few points near $D = 6$ mm.

A large number of aggregates were observed with $D \geq 1$ mm, in the quiescent cloud regions that also contained almost no liquid water. Figure 15a shows an example from Cloud 14 (22 August). In the first part of the cloud, where there was

significant liquid, the ice particles were pristine, mixed with rimed particles and some graupel. Aggregates, with an average size, $\overline{D} \approx 1$ mm, were the predominant particle type immediately after the turret, in a region of cloud with virtually no liquid. Most of the aggregates were composed of stellar crystals and were lightly rimed (Figure 15b). Aggregates were notably absent in the next slowly ascending region of cloud (Figures 15a & b). It is evident from Figure 15a that, as expected, aggregation has a clear influence on the concentration of particles observed. There is insufficient information to be able to determine why the aggregates exist where they do. However, it is likely that they will only be observed in the oldest regions of cloud since time is an important factor. It is believed that aggregation is more efficient between -12 and -17 °C because particles with dendritic features are most prominent in this temperature range. Such particles can interlock relatively easily because of their large surface area. Aggregates were frequently found near -15 °C, but also in the temperature range -10 → -20 °C. The extension of the observed "aggregation zone" to warmer temperatures is probably because aggregates can have fall speeds of 1 - 2 m s^{-1} (Locatelli and Hobbs 1974; Heymsfield 1978).

The evidence presented in this section suggested to us the following simple picture of the development of precipitation in New Mexican cumulus clouds. The clouds pass through several stages of growth and decay, gradually ascending to higher altitudes. Ice, which begins to form in the turrets near a temperature of -10 → -12 °C, will generally be transported via downdraughts to lower levels of the cloud where it may either immediately become incorporated into a new or existing updraught, or it may linger in turbulent regions near the general cloud top level. If the former is true, graupel can be produced quickly if the updraught contains substantial liquid. In the

latter situation, development of graupel must await the arrival of a fresh turret. Particles may then sediment, or in some other manner become mixed, into the updraught. In both cases there will be a sorting effect due to the variation of sizes, and hence terminal fall speeds, whereby the more numerous smaller particles will be carried upwards in the new updraught at a faster rate than the larger ones, possibly producing the pattern observed in the updraught shown in Figure 13. Once graupel particles have become embedded in the updraught, they may partake in the Hallett-Mossop process. Many secondary ice particles produced at low levels in the cloud will then be transported upwards, some to become graupel embryos, others to be carried into the anvil, or other detrainment layers.

This is a simple picture, and by no means new. Ludlam (1952), Koenig (1963), Dye et al. (1976), and Heymsfield et al. (1979) have discussed similar scenarios. The frequent supply of liquid water in fresh turrets is clearly important to the precipitation process and is probably the reason why precipitation occurs more readily in New Mexican cumulus clouds, than in clouds with similar depths in the High Plains of the United States (e.g. Cooper and Lawson 1984).

Raymond and Blyth (1989) examined a single cloud in an earlier project also located over Langmuir Lab. They found that all the trajectories of graupel particles forming the *most intense* precipitation could be traced back to a region near the tops of the cumulus congestus clouds at $T \approx -15$ °C that existed prior to the rapid development of the cloud into a thunderstorm. This result was probably due to particles that initially lingered in the cloud top region growing slowly from the relatively small amounts of liquid typical of turbulent cloud top regions, until they eventually became incorporated into the large, new turret which provided the abundant liquid required

for their growth. The details of this process is highly dependent on the magnitude and timing of the updraughts and downdraughts, and on the amount of liquid available for growth, among other factors. However, one requirement suggested from the trajectories illustrated by Raymond and Blyth (1989) is that graupel embryos be supplied to the general cloud top region. These can originate either from above, as in the initial stages of precipitation development, or also from below if secondary ice particles are produced.

Observations suggest that once ice had formed in these clouds, graupel developed rapidly. Graupel with $D \approx 2$ mm were among the first ice particles to be detected in Clouds 4 and 8 (10 and 12 August). We estimated that the 2 mm graupel formed in Cloud 8 in approximately 15 min or less; an estimate was not possible for Cloud 4. With the appropriate caveats in mind, the time from no ice to 3 mm graupel was about 15 min in Cloud 3 (9 August). Graupel did not grow to larger than 1 mm for about 30 min in Cloud 20 (28 August), since first ice was sampled at the beginning of a decay cycle of the local cloud.

Calculations of accretional growth of graupel made by Heymsfield (1982), Cooper and Lawson (1984) and Raymond and Blyth (1989) indicate that 2 - 3 mm graupel can be expected in times of 10 - 15 min if $L/L_A \approx 0.3$ - 0.5, consistent with typical values observed in clouds 3 & 4, and others. The strong dependency of the graupel growth rate upon liquid water content is evinced by the observations illustrated in Figure 13.

The actual fate of precipitation embryos is determined by what transpired after the aircraft made the measurement: the large aggregates may have remained in the

detrainment layers eventually falling to produce light rain, or they may have fallen into a liquid-laden turret. Likewise, small graupel particles may have reached their nadir at the time of measurement, and fallen without further growth also as fairly light rain. Such a situation was observed in the decaying stages of the thunderstorm discussed by Raymond and Blyth (1989).

7. SUMMARY

The main results of the study of ice particles in New Mexican cumulus clouds can be summarised as follows:

- Ice first formed, in updrafts or downdrafts, when the cloud attained a temperature of -10 → -12 ° C.
- Nucleation of first ice particles did not appear to occur preferentially in the downdrafts or in the region of cloud top.
- There were many more ice particles than studies suggest can be attributed to primary ice nucleation.
- The Hallett-Mossop process of ice splintering during riming (Hallett and Mossop 1974) is a likely candidate to explain the high concentrations of ice.
- Large drops of diameter $D \approx 1$ mm were sometimes observed just prior to the formation of ice.

The development of precipitation particles was also investigated and the main results of that study are as follows:

- There is evidence that graupel embryos are introduced into new turrets that

ascend through old cloud.

- The largest graupel particles were observed in regions containing fewer total number of particles, possibly because of particle sorting.
- Large aggregates were observed in the temperature range of -10 → -20 ° C, in regions of cloud with low liquid water content. Concentrations of individual particles were generally lower when aggregates were present.
- Ice particles often had considerable time to grow to graupel embryo sizes. A possible scenario is that ice particles are transported to the general level of cloud top (formed by stability changes in the environment) either by downdrafts, or by updrafts if they were produced at lower levels via the Hallett-Mossop process for example. Growth by vapour diffusion will usually be possible during this transport, and also during the time the particles remain in the general cloud top region. *Rapid* growth of graupel by riming must await the arrival of a fresh, liquid-laden turret. The multiple thermal nature of these clouds is therefore considered to be crucial for the development of precipitation in the New Mexcian clouds.

Acknowledgements We wish to thank the many people that were involved in the field project, particularly Dave Raymond, Bill Winn, Al Cooper, Charlie Moore, Jim Dye, Darrel Baumgardner, the late Dan Jones, the pilots of the King Air, and the folks at NCAR involved in gathering and processing the data. We would also like to thank Darrel Baumgardner for help with 2D image processing, Robert Solomon, Dinh Thon That and Shari Colella for their assistance with data analysis. We are grateful for the major support from the NSF under grants ATM-8914116 and ATM-9115694, and also the USAF under Grant No. F49620-92-J-0020, the Hadley Centre, and the NERC

under grant GR3/8377.

References

Baker, B. A., 1991: On the role of phoresis in cloud ice initiation. *J. Atmos. Sci.*, **48**, 1545 - 1548.

Baumgardner, D., 1986: Airborne measurements for cloud microphysics. NCAR Research Aviation Facility Bulletin No. 24.

Baumgardner, D., 1987: Corrections for the response times of particle measuring probes. *Sixth Symp. Meteorol. Obs. and Instruments*, New Orleans, Amer. Meteorol. Soc., 148 - 151.

Baumgardner, D., and M. Spowart, 1990: Evaluation of the Forward Scattering Spectrometer Probe. Part III: Time response and laser inhomogeneity limitations. *J. Atmos. Oceanic Tech.*, 7, 666 - 672.

Baumgardner, D., W. Strapp, and J. E. Dye, 1985: Evaluation of the Forward Scattering Spectrometer Probe. Part II: Corrections for coincidence and dead-time losses. *J. Atmos. Oceanic Tech.*, 2, 626 - 632.

Beheng, K. D., 1987: Microphysical properties of glaciating cumulus clouds: Comparison of measurements with a numerical simulation. *Quart. J. Roy. Meteorol. Soc.*, **113**, 1377 - 1382.

Blumstein, R., R. M. Rauber, L. O. Grant, and W. G. Finnegan, 1987: Application of ice nucleation kinetics in orographic clouds. *J. Clim. Appl. Meteorol.*, **26**, 1363 - 1376.

Blyth, A. M., and J. Latham, 1990: Airborne studies of the altitudinal variability of the microphysical structure of small, ice-free, Montanan cumulus clouds. *Quart. J.*

Roy. Meteorol. Soc., **116**, 1405 - 1423.

Blyth, A. M., W. A. Cooper, and J. B. Jensen, 1988: A study of the source of entrained air in Montana cumuli. *J. Atmos. Sci.*, **45**, 3944 - 3964.

Braham, Jr., R. R., 1964: What is the role of ice in summer rain-showers? *J. Atmos. Sci.*, **21**, 640 - 645.

Braham, Jr., R.R., S.E. Reynolds, and J. H. Harrel, Jr., 1951: Possibilities for cloud seeding as determined by a study of cloud height versus precipitation. *J. Meteorol.*, **8**, 416 - 418.

Brenguier, J. L., 1989: Coincidence and dead-time corrections for particle counters. Part II: High concentration measurements with an FSSP. *J. Atmos. Oceanic Tech.*, **6**, 585 - 598.

Brown, P. R. A., 1989: Use of holography for airborne cloud physics measurements. *J. Atmos. Oceanic Tech.*, **6**, 293 - 306.

Cannon, T. W., 1975: A photographic technique for measurements of atmospheric particles *in situ* from aircraft. *J. Appl. Meteorol.*, **14**, 1383 - 1388.

Cannon, T. W., J. E. Dye, and V. Toutenhoofd, 1974: The mechanism of precipitation formation in northeastern Colorado cumulus II. Sailplane measurements. *J. Atmos. Sci.*, **31**, 2148 - 2151.

Caylor, I.J., A.J. Illingworth, 1987: Radar observations and modelling of warm rain initiation. *Quart. J. Roy. Meteor. Soc.*, **113**, 1171 - 1191.

Cerni, T. A., 1983: Determination of the size and concentration of cloud drops with an FSSP. *J. Climate Appl. Meteorol.*, **22**, 1346 - 1355.

Chisnell, R. F., and J. Latham, 1976: Ice particle multiplication in cumulus clouds. *Quart. J. Roy. Meteorol. Soc.*, **102**, 133 - 156.

Cooper, W. A., 1986: Ice initiation in natural clouds. Pp 29-32 in *Precipitation enhancement - a scientific challenge*. R. R. Braham, Jr., Ed., *Meteor. Mon.*, **21**.

Cooper, W. A., 1988: Effects of coincidence on measurements with a forward scattering spectrometer probe. *J. Atmos. Oceanic Tech.*, **5**, 823 - 832.

Cooper, W. A., and C. P. R. Saunders, 1980: Winter storms over the San Juan Mountains. PartII: Microphysical processes. *J. Appl. Meteorol.*, **19**, 927 - 941.

Cooper, W. A., and G. Vali, 1981: The origin of ice in mountain cap clouds. *J. Atmos. Sci.*, **38**, 1244 - 1259.

Cooper, W. A., and R. P. Lawson, 1984: Physical interpretation of results from HIPLEX-1 Experiment. *J. Climate Appl. Meteorol.*, **23**, 532 - 540.

Dong, Y. Y., and J. Hallett, 1989: Droplet accretion during rime growth and the formation of secondary ice crystals. *Quart. J. Roy. Meteorol. Soc.*, **115**, 127 - 142.

Dye, J. E., 1983: The microphysical structure of the 7 August 1979 New Mexico thunderstorm. Pp. 304-307 in *Proceedings in atmospheric electricity*. L.H. Rhunke and J. Latham, Eds., Deepak Publishing.

Dye, J. E., and D. Baumgardner, 1984: Evaluation of the forward scattering spectrometer probe. Part I: Electronic and optical studies. *J. Atmos. Oceanic Tech.*, **1**, 329 - 344.

Dye, J. E., C. A. Knight, V. Toutenhoofd, and T. W. Cannon, 1974: The mechanism of precipitation formation in northeastern Colorado cumulus III. Coordinated microphysical and radar observations and summary. *J. Atmos. Sci.*, **31**, 2152 -

2159.

Dye, J. E., J. J. Jones, A. J. Weinheimer, and W. P. Winn, 1988: Observations within two regions of charge during initial thunderstorm electrification. *Quart. J. Roy. Meteorol. Soc*, **114**, 1271 - 1290.

Dye, J. E., C. A. Knight, P. N. Johnson, T. W. Cannon, and V. Toutenhoofd, 1976: Observations of the development of precipitation-sized ice particles in NE Colorado thunderstorms. *Preprints International Conference on Cloud Physics* , Boulder, USA, 478 - 483.

Dye, J. E., J. J. Jones, W. P. Winn, T. A. Cerni, B. Gardiner, D. Lamb, R. L. Pitter, J. Hallett, and C. P. R. Saunders, 1986a: Early electrification and precipitation development in a small, isolated Montana cumulonimbus. *J. Geophys. Res.*, **91**, D1, 1231-1247.

_____, 1986b: Correction (to above article). *J. Geophys. Res.*, 91 (D6), 6747 - 6750.

Fletcher, N. H., 1962: *The Physics of Rainclouds*. Cambridge Press. 390 pp.

Gagin, A. 1975: The ice phase in winter continental cumulus clouds. *J. Atmos. Sci.*, **32**, 1604 - 1614.

Gamache, J. F., 1990: Microphysical observations in summer MONEX convective and stratiform clouds. *Mon. Weather Rev.*, **118**, 1238 - 1249.

Gardiner, B. A., and J. Hallett, 1985: Degradation of in-cloud forward scattering spectrometer probe measurements in the presence of ice particles. *J. Atmos. Oceanic Tech.*, 2, 171 - 180.

Gokhale, N. R., and J. Goold, Jr., 1968: Droplet freezing by surface nucleation. *J. Appl. Meteorol.*, 7, 870 - 874.

Hallett, J., and S. C. Mossop, 1974: Production of secondary ice particles during the riming process. *Nature*, **249**, 26-28.

Hallett, J., R. I. Sax, D. L. Lamb, and A. S. Ramachandra Murty, 1978: Aircraft measurements of ice in Florida cumuli. *Quart. J. Roy. Meteorol. Soc.*, **104**, 631 - 651.

Harris-Hobbs, R. L., and W. A. Cooper, 1987: Field evidence supporting quantitative predictions of secondary ice production rates. *J. Atmos. Sci.*, **44**, 1071 - 1082.

Heymsfield, A. J., 1978: The characteristics of graupel particles in northeast Colorado cumulus congestus clouds. *J. Atmos. Sci.*, **35**, 284 - 295.

Heymsfield, A. J., 1982: A comparative study of the rates of development of potential graupel and hail embryos in High Plains storms. *J. Atmos. Sci*, **39**, 2867 - 2897.

Heymsfield, A. J., C. A. Knight, and J. E. Dye, 1979: Ice initiation in unmixed updraft cores in northeast Colorado cumulus congestus clouds. *J. Atmos. Sci.*, **36**, 2216-2229.

Hobbs, P. V., and A. J. Alkezweeny, 1968: The fragmentation of freezing water droplets in free fall. *J. Atmos. Sci.*, **25**, 881 - 888.

Hobbs, P. V., and D. A. Atkinson, 1976: The concentrations of ice particles in orographic clouds and cyclonic storms over the Cascade mountains. *J. Atmos. Sci*, **33**, 1362 - 1374.

Hobbs, P. V., and A. L. Rangno, 1985: Ice particle concentrations in clouds. *J. Atmos. Sci.*, **42**, 2523 - 2549.

Hobbs, P. V., Politovich, M. K., and L. F. Radke, 1980: The structure of summer convective clouds in eastern Montana. I: Natural Clouds. *J. Appl. Meteorol.*, **19**, 645

- 663.

Jayaweera, K. O. L. F., and T. Ohtake, 1973: Concentrations of ice crystals in Arctic stratus clouds. *J. Rech. Atmos.*, 7, 199 - 207.

Keller, V. W., and R. I. Sax, 1981: Microphysical development of a pulsating cumulus tower: a case study. *Quart. J. Roy. Meteorol. Soc.*, 107, 679 - 697.

King, W. D., D. A. Parkin, and R. J. Handsworth, 1978: A hot-wire liquid water device having fully calculable response characteristics. *J. Appl. Meteorol.*, 17, 1809 - 1813.

Knight, C. A., N. C. Knight, J. E. Dye, and V. Toutenhoofd, 1974: The mechanism of precipitation formation in northeastern Colorado cumulus I. Observations of the precipitation itself. *J. Atmos. Sci.*, 31, 2142 - 2147.

Knollenberg, R. G., 1970: The optical array: An alternative to extinction and scattering for particle size measurement. *J. Appl. Meteorol.*, 9, 86 - 103.

Knollenberg, R. G., 1976: Three new instruments for cloud physics measurements: The 2-D spectrometer, the forward scattering spectrometer probe, and the active scattering aerosol spectrometer. Preprints *Int. Conf. on Cloud Physics*, Boulder, Amer. Meteorol. Soc. 554 - 561.

Knollenberg, R. G., 1981: Techniques for probing cloud microstructure *Clouds, Their Formation, Optical Properties, and Effects*. P. V. Hobbs, A. Deepak, Eds. Academic Press, 495 pp.

Koenig, L. R., 1963: The glaciating behavior of small cumulonimbus clouds. *J. Atmos. Sci.*, 20, 29-47.

Lawson, R. P., and W. A. Cooper, 1990: Performance of some airborne thermometers in clouds. *J. Atmos. Oceanic Tech.*, **7**, 480 - 494.

Lenschow, D. H., and P. Spyers-Duran, 1987: Measurement techniques: Air motion sensing. NCAR research aviation facility Bulletin No. 23.

Locatelli, J. D., and P. V. Hobbs, 1974: Fall speeds and masses of solid precipitation particles. *J. Geophys. Res.*, **79**, 2185 - 2197.

Ludlam, F. H., 1952: The production of showers by the growth of ice particles. *Quart. J. Roy. Meteorol. Soc.*, **78**, 543 - 553.

Mason, B.J., and P.R. Jonas, 1974: The evolution of droplet spectra and large droplets by condensation in cumulus clouds. *Quart. J. R. Meteor. Soc.*, **100**, 23 - 38.

Miller, L. J., J. D. Tuttle, and C. A. Knight, 1988: Airflow and hail growth in a severe northern high plains supercell. *J. Atmos. Sci.*, **45**, 736 - 762.

Mossop, S. C., 1968: Comparison between concentration of ice crystals in cloud and the concentration of ice nuclei. *J. Rech. Atmos.*, **3**, 119 - 124.

Mossop, S. C., 1970: Concentrations of ice crystals in clouds *Bull. Amer. Meteor. Soc.*, **51**, 474-478.

Mossop, S. C., 1976: Production of secondary ice particles during the growth of graupel by riming. *Quart. J. Roy. Meteorol. Soc.*, **102**, 45 - 57.

Mossop, S. C., 1978: Some factors governing ice particle multiplication in cumulus clouds. *J. Atmos. Sci.*, **35**, 2033 - 2037.

Mossop, S. C., 1985a: The origin and concentration of ice crystals in clouds. *Bull. Amer. Meteor. Soc.*, **66**, 264-273.

Mossop, S. C., 1985b: Microphysical properties of supercooled cumulus clouds in which an ice particle multiplication process operated. *Quart. J. Roy. Meteorol. Soc.*, **111**, 183 - 198.

Mossop, S. C., 1985c: Secondary ice particle production during rime growth: the effect of drop size distribution and rimer velocity. *Quart. J. Roy. Meteorol. Soc*, **111**, 1113 - 1124.

Mossop, S. C., and A. Ono, 1969: Measurements of ice crystal concentration in clouds. *J. Atmos. Sci.*, **26**, 130 - 137.

Mossop, S. C., and J. Hallett, 1974: Ice crystal concentration in cumulus clouds: influence of the drop spectrum. *Science*, **186**, 632 - 634.

Mossop, S. C., R. E. Cottis, and B. M. Bartlett, 1972: Ice crystal concentrations in cumulus and stratocumulus clouds. *Quart. J. Roy. Meteorol. Soc.*, **98**, 105 - 123.

Pruppacher, H. R., and J. D. Klett, 1980: *Microphysics of Clouds and Precipitation*, Reidel Pub. Co., Holland.

Rangno, A. L., and P. V. Hobbs, 1983: Production of ice particles in clouds due to aircraft penetrations. *J. Clim. Appl. Meteorol.*, **22**, 214 - 232.

Rangno, A. L., and P. V. Hobbs, 1991: Ice particle concentrations and precipitation development in small polar maritime cumuliform clouds. *Quart. J. Roy. Meteorol. Soc.*, **117**, 207 - 241.

Raymond, D. J., and M. H. Wilkening, 1982: Flow and mixing in New Mexico mountain cumuli. *J. Atmos. Sci.*, **39**, 2211 - 2228.

Raymond, D. J., and M. Wilkening, 1985: Characteristics of mountain-induced thunderstorms and cumulus congestus clouds from budget measurements. *J. Atmos.*

Sci., **42**, 773 - 783.

Raymond, D. J., and A. M. Blyth, 1989: Precipitation development in a New Mexico thunderstorm. *Quart. J. Roy. Meteor. Soc.*, **115**, 1397-1423.

Raymond, D. J., R. Solomon, and A. M. Blyth, 1991: Mass fluxes in New Mexico mountain thunderstorms from radar and aircraft measurements. *Quart. J. Roy. Meteorol. Soc.*, **117**, 587 - 621.

Research Aviation Facility, 1990: The King Air: Overview and summary capabilities. NCAR Research Aviation Facility Bulletin No. 2.

Rodi, A.R., and P. A. Spyers-Duran, 1972: Analysis of time response of airborne temperature sensors. *J. Appl. Meteor.*, **11**, 554 - 556.

Roesner, S., A. I. Flossmann, and H. R. Pruppacher, 1990: The effect on the evolution of the drop spectrum in clouds of the preconditioning of air by successive convective elements. *Quart. J. Roy. Meteorol. Soc.*, **116**, 1389 - 1403.

Rogers. D. C., 1982: Field and laboratory studies of ice nucleation in winter orographic clouds. Ph.D. dissertation, University of Wyoming, 161 pp.

Rosinski, J., and G. Morgan, 1991: Cloud condensation nuclei as a source of ice-forming nuclei in clouds. *J. Aerosol Sci.* , **22**, 123 - 133.

Ryan, B. F., E. R. Wishart, and D. E. Shaw, 1976: The growth rates and densities of ice crystals between -3°C and -21°C. *J. Atmos. Sci.*, **33**, 842 - 850.

Spyers-Duran, P. A., 1968: Comparative measurements of cloud liquid water using heated wire and cloud replicating devices. *J. Appl. Meteorol.*, **7**, 674 - 678.

Strapp, J.W., and R.S. Schemenauer, 1982: Calibrations of Johnson-Williams liquid

water content meters in a high speed icing tunnel. *J. Appl. Meteor.*, **21**, 98 - 108.

Warner, J., 1969: The microstructure of cumulus cloud. Part I. General features of the droplet spectrum. *J. Atmos. Sci.*, **26**, 1049 - 1059.

Winn, W. P., C. B. Moore, C. R. Holmes, and L. G. Byerley, 1978: Thunderstorm on July 16, 1975, over Langmuir Laboratory: a case study. *J. Geophys. Res.*, **83**, 3079 - 3092.

Young, K. C., 1974: The role of contact nucleation in ice phase initiation in clouds. *J. Atmos. Sci.*, **31**, 768-776.

FIGURE CAPTIONS

Fig. 1: Cloud droplet spectra measured by the FSSP at approximate altitudes of 0.6, 1.3, and 2.5 km above cloud base (labelled A, B, and C respectively) in Cloud 4, 10 August, 1987. Each spectrum is an average over the whole penetration.

Fig. 2a: Vertical wind, w plotted against altitude above cloud base, z for all penetrations through Cloud 3, 9 August, 1987. The vertical bars close to the $w = 0$ m s^{-1} line represent the penetration average values.

Fig. 2b: Vertical wind, w, plotted against altitude above cloud base, z, for all cumulus clouds in the project.

Fig. 3: The bottom three panels from top to bottom respectively, are concentration of particles measured by the 2DC (N_C) and 1D (N_X) probes, and liquid water content derived from the FSSP (L). The uppermost panel is the vertical wind (w) superimposed with wind vectors constructed from the horizontal component along the track of the aircraft and the vertical wind. All graphs are plotted against time: 10 seconds is approximately 1 km of flight. Data are from a penetration where $T \approx$ -7 °C, made towards the upwind side of Cloud 3 on 9 August, 1987 at 1257 MDT.

Fig. 4: Flux, F (vertical wind times concentration) of ice particles of diameter, $D <$ 500 μm plotted against the normalised distance across the cloud, X. The normalised distance is the distance across the cloud, normalised to unity, commencing on the upshear side in a, d, e & f when penetrations were made parallel to the

wind. Penetrations were made across wind in b & c. The plots are: a - Cloud 1, 8 August; b - Cloud 3a, 9 August; c - Cloud 3b, 9 August; d - Cloud 4, 10 August; e - Cloud 8, 12 August; f - Cloud 20, 28 August.

Fig. 5: Penetration made in Cloud 9, at 1312 MDT, 19 August, 1987 where $T \approx$ -13 °C. The bottom three panels are concentration of particles measured by, in descending order, the 2DP (N_P), 2DC (N_C) and 1D (N_X) probes. The top panel is the vertical (w), and horizontal wind - see caption to Fig. 3. 10 seconds is approximately 1 km of flight.

Fig. 6: Vertical wind, w, versus maximum size of particle detected by the 2DC in 10 m of flight, D_{Cmax} for a penetration on 22 August, 1987. The temperature at the observation level was $T \approx$ -15 °C.

Fig. 7: Maximum concentration of ice particles detected by the 2DC (N_{Cmax}) in the penetration in which ice was first detected, versus temperature, T. The temperature at both cloud top (+) at the time of the measurement and the penetration level (*) are indicated. The points with the vertical bars above and below are taken from Cooper (1986) and the dashed line is the Fletcher nucleation curve.

Fig. 8: As Fig. 7, but for maximum concentration of *all* particles measured by the 2DC in all the clouds. The cloud top temperature is the minimum up to the time the maximum concentration was measured.

Fig. 9: Cloud droplet spectra measured by the FSSP between temperatures -3 → -8 °C: solid line is the average spectrum for all clouds, other than Cloud 9, 19

August, and the dashed line is for Cloud 9.

Fig. 10: Flux, F (vertical wind times concentration) of ice particles of diameter, $D <$ 500 μm plotted against the normalised distance across the cloud, X, for only isolated turrets containing updraughts. The normalised distance is the distance across the cloud, normalised to unity, commencing on the upshear side.

Fig. 11a: Concentration of particles measured by the 2DC, N_C, versus temperature, T, for regions of cloud with vertical wind, w either greater than 3 m s^{-1} (□), or less than -3 m s^{-1} (×). Values are 1 Hz. For those regions with $w > 3$ m s^{-1}, samples are limited to those with an average particle diameter $\overline{D} > 500$ μm. Samples with $N_C = 0$ are not plotted.

Fig. 11b: Same as Fig. 11a but for $-3 < w < 3$ m s^{-1}, and all sizes of particles.

Fig. 12a: Concentration of all particles of size $D \geq 3$ mm measured by the 2DP, N_{3P}, versus ratio of liquid water content to the adiabatic value, L/L_A for regions of cloud with vertical wind, w either greater than 3 m s^{-1} (□), or less than -3 m s^{-1} (×). Samples are 1 Hz, and those with $N_{3P} = 0$ are not plotted.

Fig. 12b: Same as Fig. 12a, but for $-3 < w < 3$ m s^{-1}.

Fig. 13: Plot of vertical (w) and horizontal wind, average size of particles detected by the 2DP in 0.1 s ($\overline{D_P}$), concentration of particles detected by the 2DP (N_P), and liquid water content measured by the Johnson-Williams device L, from top to bottom respectively, for Cloud 14, 22 August, 1987. The temperature was

approximately -12.5 °C. Gaps in the graph of $\overline{D_p}$ are due to overload of the probe.

Fig. 14: Concentration of particles detected by the 2DC, N_C, versus the maximum size of particles detected by the 2DP in 0.1 s, D_{Pmax}, for regions of cloud with JW liquid water content greater than 0.1 g m^{-3}. The entire set of cumulus clouds are used.

Fig. 15a: Vertical (w) and horizontal wind, liquid water content measured by the Johnson-Williams device (L), maximum size in 0.1 s (D_{Pmax}) and concentration (N_P) of particles detected by the 2DP, from top to bottom respectively for Cloud 14, 22 August, 1987. The temperature was approximately -14 °C. The gaps in the graph of D_{Pmax} are caused by overloading of the probe.

Fig. 15b: 2D images from the 2DC and 2DP probes from the regions of cloud indicated by **A** and **B** in Figure 15a. The text under each strip of images refers to the probe, date, and beginning and end time of the images. The distance between the horizontal lines is approximately 800 and 6400 μm for the 2DC and 2DP probes respectively.

Table 1. Approximate size range, resolution and sample volume of the four Particle Measuring Systems probes on board the King Air.

Instrument	FSSP	1D (200X)	2DC	2DP
Size Range (μm)	0.5 - 50	20 - 280	25 - 800	200 - 6400
Resolution (μm)	0.5 - 3	20	25	200
Sample Volume per 100 m	15 cm^3	~0.5 L	~5 L	~168 L

Table 2. Information concerning New Mexican cumulus clouds studied during August, 1987. The ice particle concentrations in column 9 are from the 2DC.

Date	Cloud No.	Times of penetrations	Base temp, pres (°C, mb)	Temp of max top (°C)	Range of penetration temp (°C)	Max drop conc (cm^{-3})	Max vertical wind ($m\ s^{-1}$)	Max ice particle conc (L^{-1})
8	1	1657-1854	9.0, 670	-13	5.2 → -9.7	598	9.8	1.1
9	2	1651-1714	7.4, 665	-10*	7.4 → -3.3	311	1.0	18.1
9	3	1739-1923	7.4, 665	-15*	3.4 → -6.9	597	12.0	38.1
10	4	1756-1934	10.6, 705	-15	6.6 → -9.3	513	10.5	158.1
11	5	1722-1735	6.2, 640	-12	-8.0 → -10.1	586	6.3	31.3
11	6	1744-1900	6.2, 640	-15	-9.7 → -14.6	570	5.2	255.1
12	7	1849-1900	7.1, 664	-4	3.0 → -2.9	553	5.9	0 †
12	8	1903-2021	7.1, 664	-17*	-4.5 → -15.0	573	9.4	268.0
19	9	1833-2007	1.0, 598	-16	-8.7 → -13.9	676	8.8	44.0
20	10	1851-1918	4.8, 620	-17	-8.4 → -15.3	575	6.6	170.4
20	11	1928-2001	4.8, 620	-15	1.6 → -8.6	726	6.8	3.7
20	12	2016-2042	4.8, 620	-19	-3.4 → -15.6	665	8.6	9.6
21	13	1718-1754	6.0, 648	-13	1.2 → -8.3	713	16.6	6.8
22	14	1828-1909	5.0, 655	-19	-11.9 → -16.1	708	10.5	398.3
27	15	1703-1724	3.9, 690	-26	-16.5 → -23.6	78	4.7	1299.2
27	16	1734-1750	3.9, 690	-27	-18.8 → -21.6	484	5.2	510.6
27	17	1843-1858	3.9, 690	-16	-9.4 → -11.4	635	5.6	11.0
27	18	1900-1920	3.9, 690	-15	-9.3 → -10.3	555	5.6	698.8
28	19	1750-1755	6.5, 700	-8	-6.2 → -7.2	420	5.8	0 †
28	20	1801-1938	6.5, 700	-13	-3.6 → -11.3	649	14.2	43.6 ‡

* Estimate

† A few small indistinguishable particles were observed.

‡ Maximum concentration measured before 2DC probe failed

Table 3. Cases where first ice formed during the study. Cloud number corresponds to entries in Table 2. The times are when ice particles were first observed by the 2DC or 2DP probe. T, and T_{ct} are respectively temperatures at the penetration level and cloud top; N_{Cmax} is the maximum concentration of ice particles measured by the 2DC probe in about 100 m of cloud during the penetration. The entries a and b for 9 August are for separate turrets of the same cloud, while the entry Cloud 2 corresponds to a cloud studied earlier on the same day.

Date (Aug)	Cloud No.	Time (GMT)	T (°C)	T_{ct} (°C)	N_{Cmax} (L^{-1})
8	1	1853	-9.7	-13	1.1
9	2	1707	-3.3	-10	4.0‡
9a	3	1857	-6.9	-15*	20.7†
9b	3	1923	-5.7	-12	10.0†
10	4	1925	-8.5	-15	44.0†
12	8	1924	-8.3	-15*	0.6
28	20	1832	-11.3	-13	0.3

* Only an estimate due to overhanging cloud

† mm-sized drops observed prior to ice particle formation

‡ Most particles were mm-sized drops at this time

FIGURE CAPTIONS

Fig. 1: Cloud droplet spectra measured by the FSSP at approximate altitudes of 0.6, 1.3, and 2.5 km above cloud base (labelled A, B, and C respectively) in Cloud 4, 10 August, 1987. Each spectrum is an average over the whole penetration.

Fig. 2a: Vertical wind, w plotted against altitude above cloud base, z for all penetrations through Cloud 3, 9 August, 1987. The vertical bars close to the $w = 0$ m s^{-1} line represent the penetration average values.

Fig. 2b: Vertical wind, w, plotted against altitude above cloud base, z, for all cumulus clouds in the project.

Fig. 3: The bottom three panels from top to bottom respectively, are concentration of particles measured by the 2DC (N_C) and 1D (N_X) probes, and liquid water content derived from the FSSP (L). The uppermost panel is the vertical wind (w) superimposed with wind vectors constructed from the horizontal component along the track of the aircraft and the vertical wind. All graphs are plotted against time: 10 seconds is approximately 1 km of flight. Data are from a penetration where $T \approx$ -7 °C, made towards the upwind side of Cloud 3 on 9 August, 1987 at 1257 MDT.

Fig. 4: Flux, F (vertical wind times concentration) of ice particles of diameter, $D <$ 500 μm plotted against the normalised distance across the cloud, X. The normalised distance is the distance across the cloud, normalised to unity, commencing on the upshear side in a, d, e & f when penetrations were made parallel to the

wind. Penetrations were made across wind in b & c. The plots are: a - Cloud 1, 8 August; b - Cloud 3a, 9 August; c - Cloud 3b, 9 August; d - Cloud 4, 10 August; e - Cloud 8, 12 August; f - Cloud 20, 28 August.

Fig. 5: Penetration made in Cloud 9, at 1312 MDT, 19 August, 1987 where $T \approx -13$ °C. The bottom three panels are concentration of particles measured by, in descending order, the 2DP (N_P), 2DC (N_C) and 1D (N_X) probes. The top panel is the vertical (w), and horizontal wind - see caption to Fig. 3. 10 seconds is approximately 1 km of flight.

Fig. 6: Vertical wind, w, versus maximum size of particle detected by the 2DC in 10 m of flight, D_{Cmax} for a penetration on 22 August, 1987. The temperature at the observation level was $T \approx -15$ °C.

Fig. 7: Maximum concentration of ice particles detected by the 2DC (N_{Cmax}) in the penetration in which ice was first detected, versus temperature, T. The temperature at both cloud top (+) at the time of the measurement and the penetration level (*) are indicated. The points with the vertical bars above and below are ~~taken from Cooper (1986)~~ and the dashed line is the Fletcher nucleation curve.

Fig. 8: As Fig. 7, but for maximum concentration of *all* particles measured by the 2DC in all the clouds. The cloud top temperature is the minimum up to the time the maximum concentration was measured.

Fig. 9: Cloud droplet spectra measured by the FSSP between temperatures -3 → -8 °C: solid line is the average spectrum for all clouds, other than Cloud 9, 19

August, and the dashed line is for Cloud 9.

Fig. 10: Flux, F (vertical wind times concentration) of ice particles of diameter, $D <$ 500 μm plotted against the normalised distance across the cloud, X, for only isolated turrets containing updraughts. The normalised distance is the distance across the cloud, normalised to unity, commencing on the upshear side.

Fig. 11a: Concentration of particles measured by the 2DC, N_C, versus temperature, T, for regions of cloud with vertical wind, w either greater than 3 m s^{-1} (□), or less than -3 m s^{-1} (×). Values are 1 Hz. For those regions with $w >$ 3 m s^{-1}, samples are limited to those with an average particle diameter $\overline{D} >$ 500 μm. Samples with $N_C = 0$ are not plotted.

Fig. 11b: Same as Fig. 11a but for $-3 < w < 3$ m s^{-1}, and all sizes of particles.

Fig. 12a: Concentration of all particles of size $D \geq 3$ mm measured by the 2DP, N_{3P}, versus ratio of liquid water content to the adiabatic value, L/L_A for regions of cloud with vertical wind, w either greater than 3 m s^{-1} (□), or less than -3 m s^{-1} (×). Samples are 1 Hz, and those with $N_{3P} = 0$ are not plotted.

Fig. 12b: Same as Fig. 12a, but for $-3 < w < 3$ m s^{-1}.

Fig. 13: Plot of vertical (w) and horizontal wind, average size of particles detected by the 2DP in 0.1 s ($\overline{D_P}$), concentration of particles detected by the 2DP (N_P), and liquid water content measured by the Johnson-Williams device L, from top to bottom respectively, for Cloud 14, 22 August, 1987. The temperature was

approximately -12.5 °C. Gaps in the graph of $\overline{D_p}$ are due to overload of the probe.

Fig. 14: Concentration of particles detected by the 2DC, N_C, versus the maximum size of particles detected by the 2DP in 0.1 s, D_{Pmax}, for regions of cloud with JW liquid water content greater than 0.1 g m^{-3}. The entire set of cumulus clouds are used.

Fig. 15a: Vertical (w) and horizontal wind, liquid water content measured by the Johnson-Williams device (L), maximum size in 0.1 s (D_{Pmax}) and concentration (N_P) of particles detected by the 2DP, from top to bottom respectively for Cloud 14, 22 August, 1987. The temperature was approximately -14 °C. The gaps in the graph of D_{Pmax} are caused by overloading of the probe.

Fig. 15b: 2D images from the 2DC and 2DP probes from the regions of cloud indicated by A and B in Figure 15a. The text under each strip of images refers to the probe, date, and beginning and end time of the images. The distance between the horizontal lines is approximately 800 and 6400 μm for the 2DC and 2DP probes respectively.

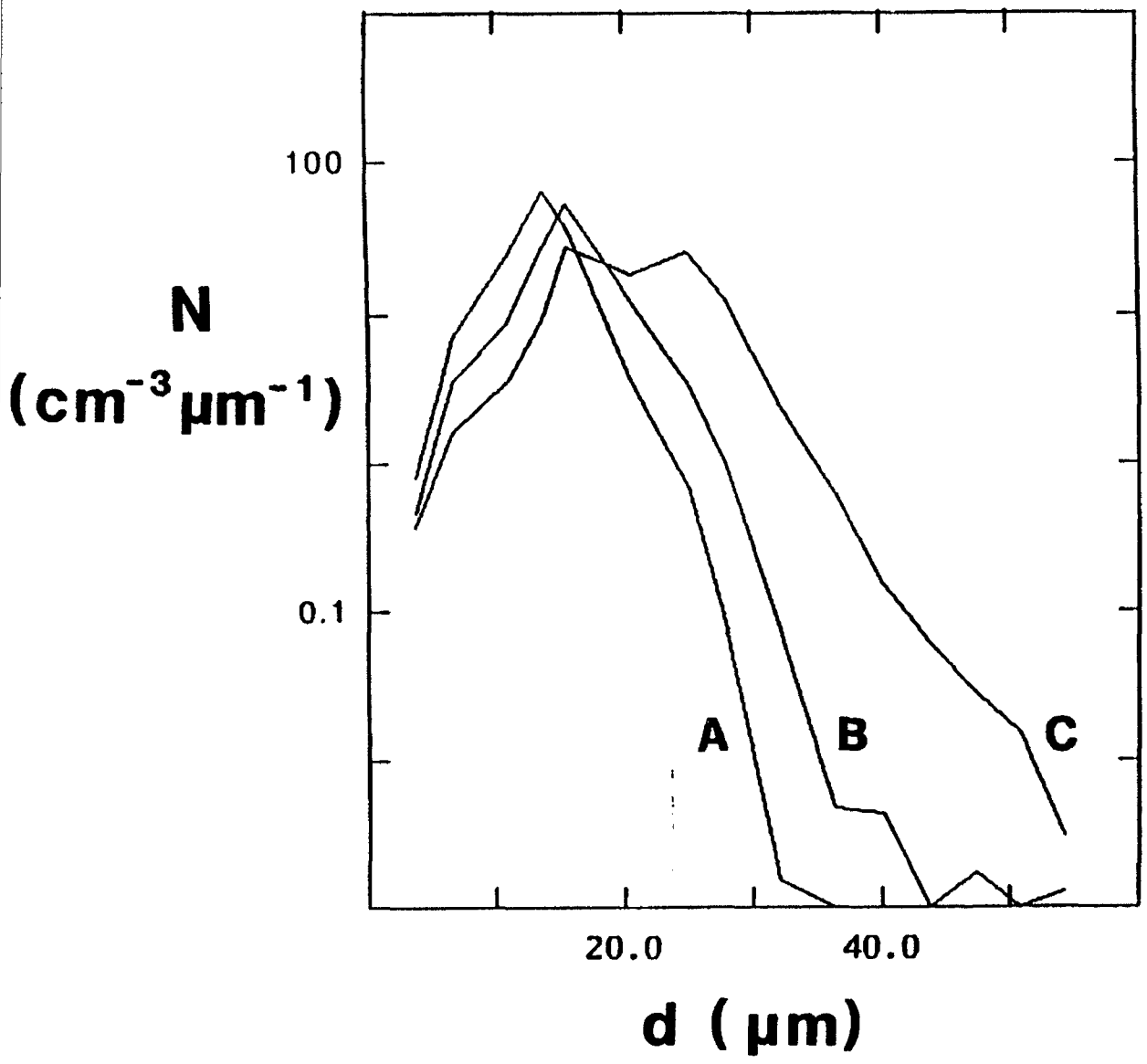
100
0.1
N
(cm⁻³μm⁻¹)
A
B
C
20.0
40.0
d (μm)

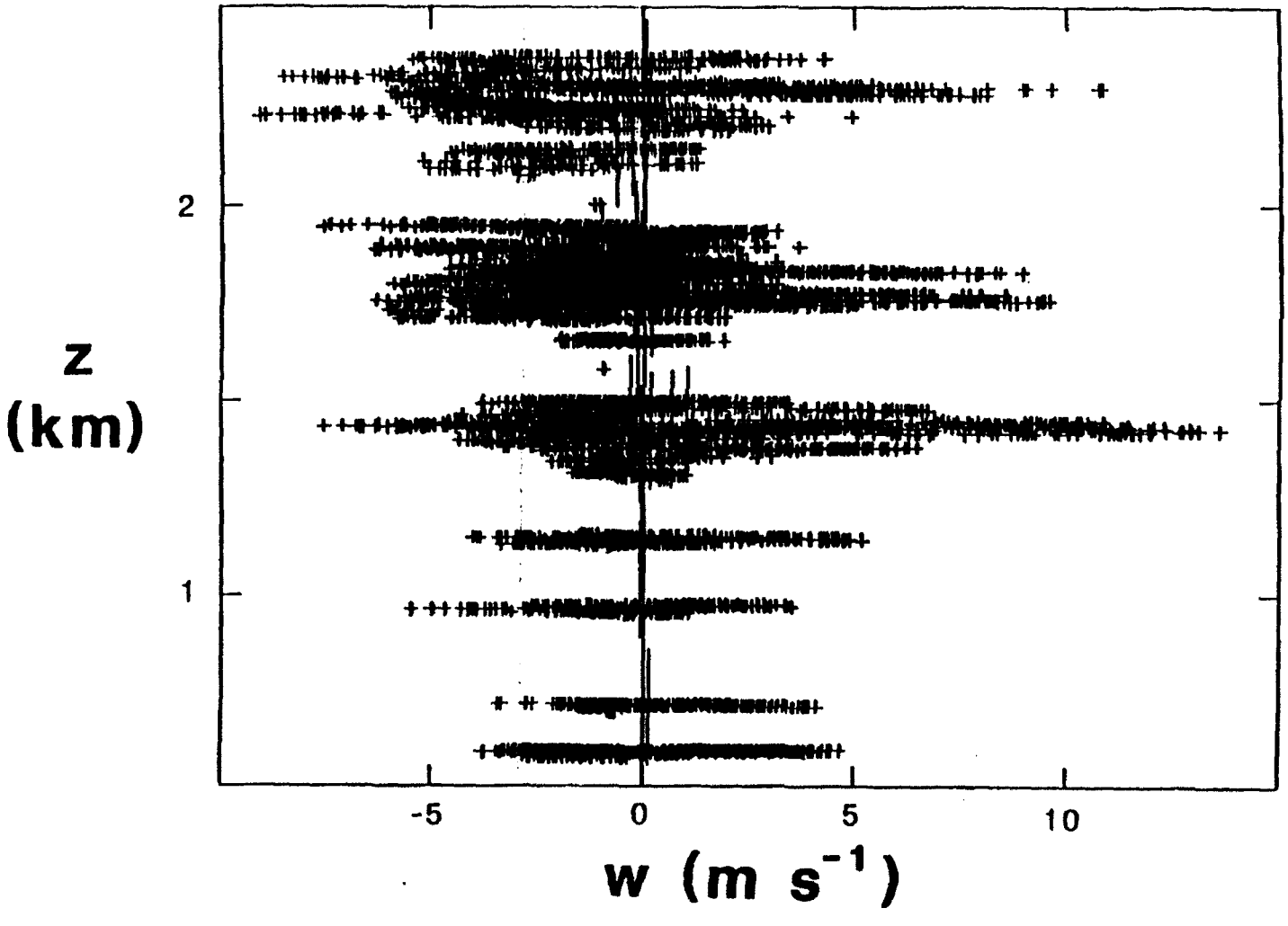
z
(km)
2
1
-5
0
5
10
w (m s-1)

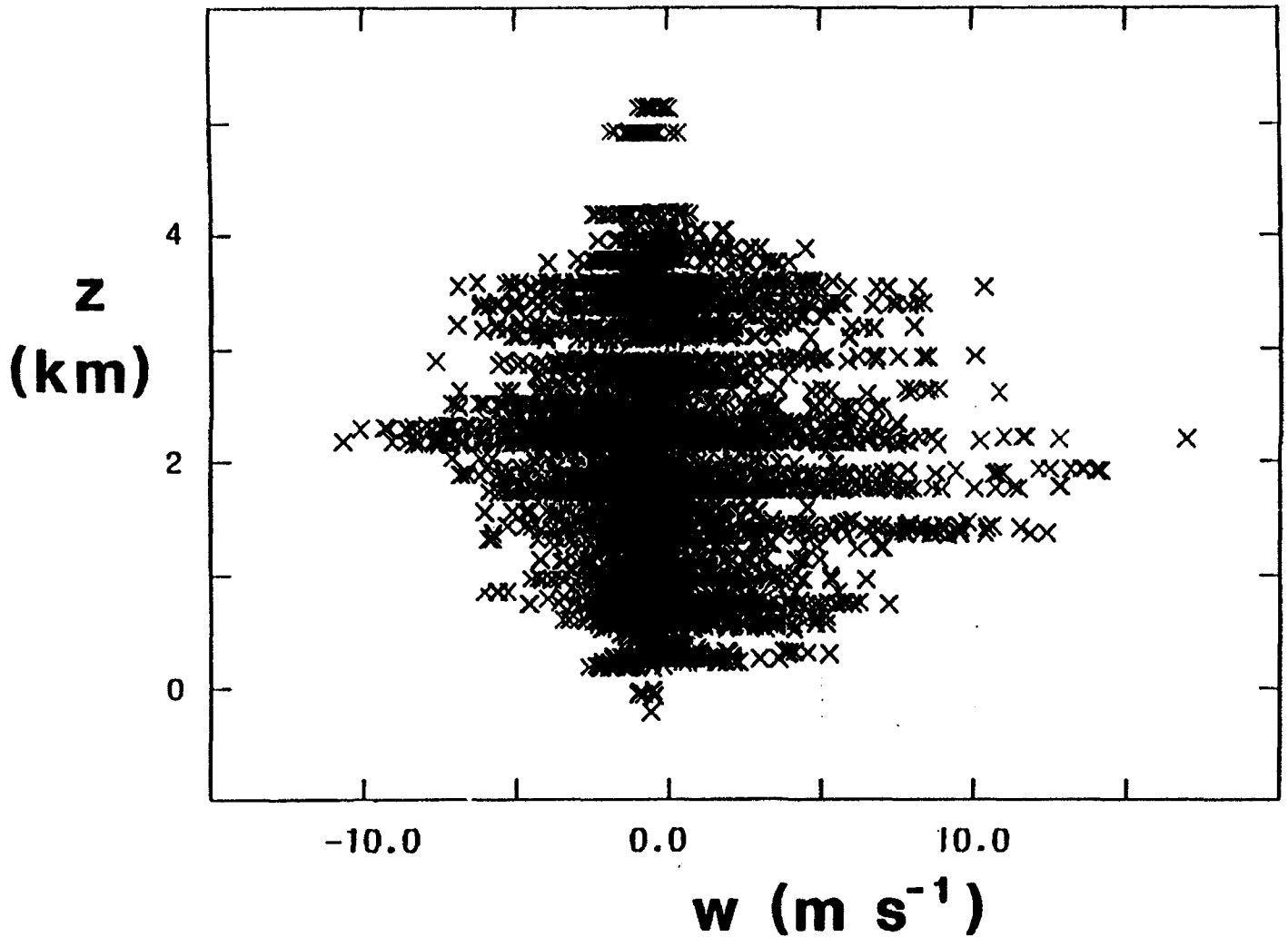
z
(km)
4
2
0
-10.0
0.0
10.0
w (m s-1)

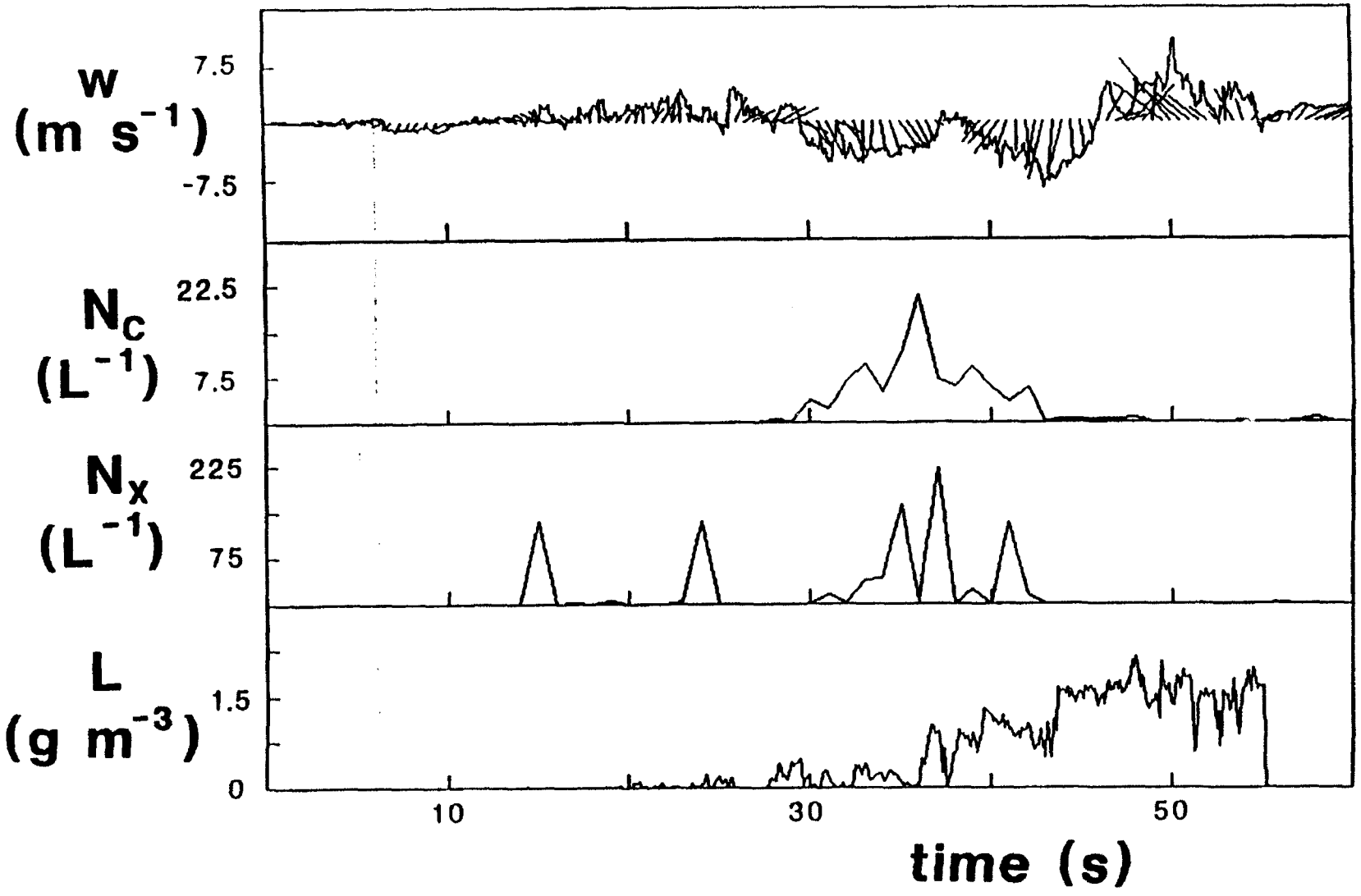
w
(m s^{-1})
7.5
-7.5
N_C
(L^{-1})
22.5
7.5
N_X
(L^{-1})
225
75
L
(g m^{-3})
1.5
0
10
30
50
time (s)

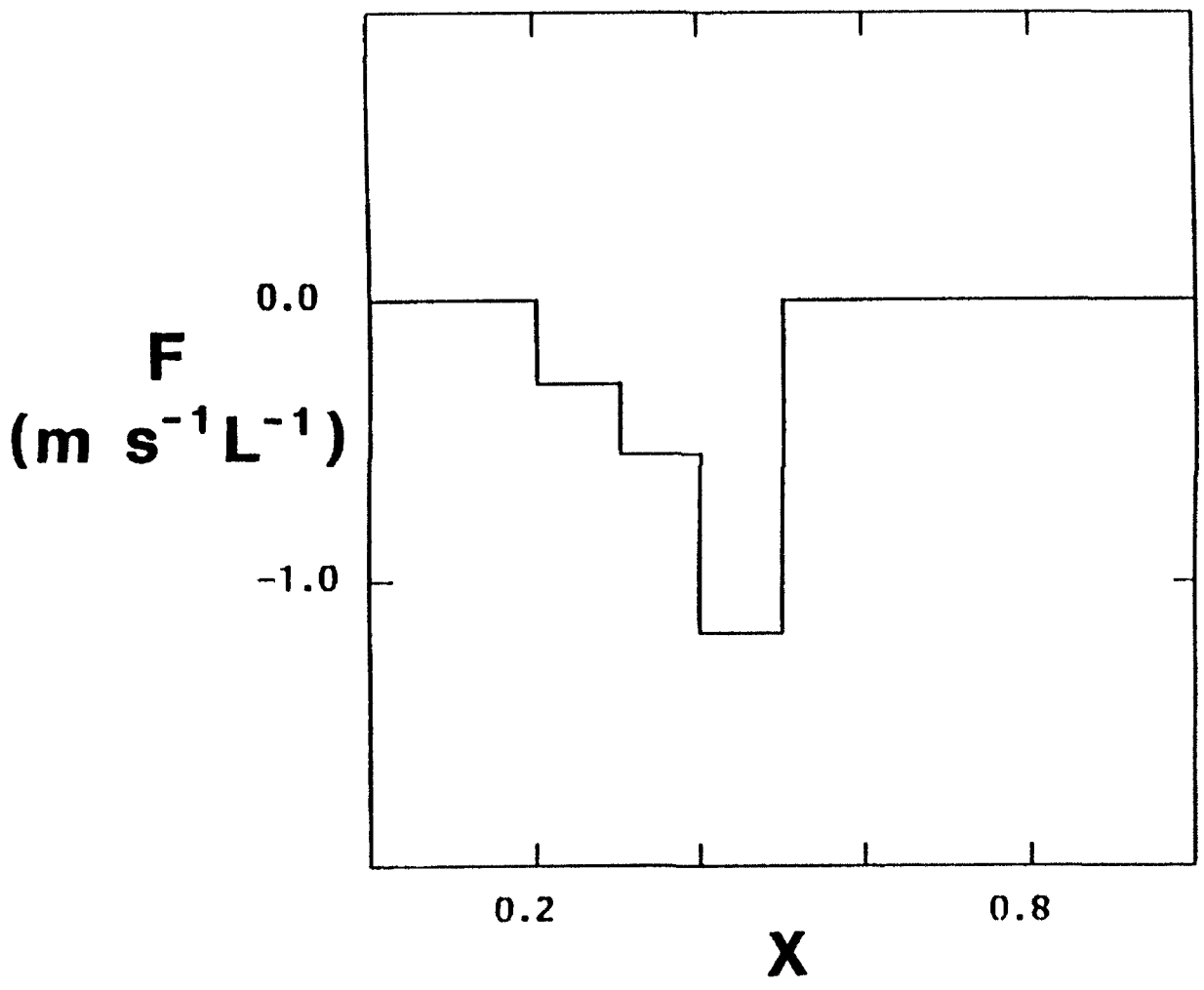
0.0
F
(m s^{-1}L^{-1})
-1.0
0.2
0.8
X

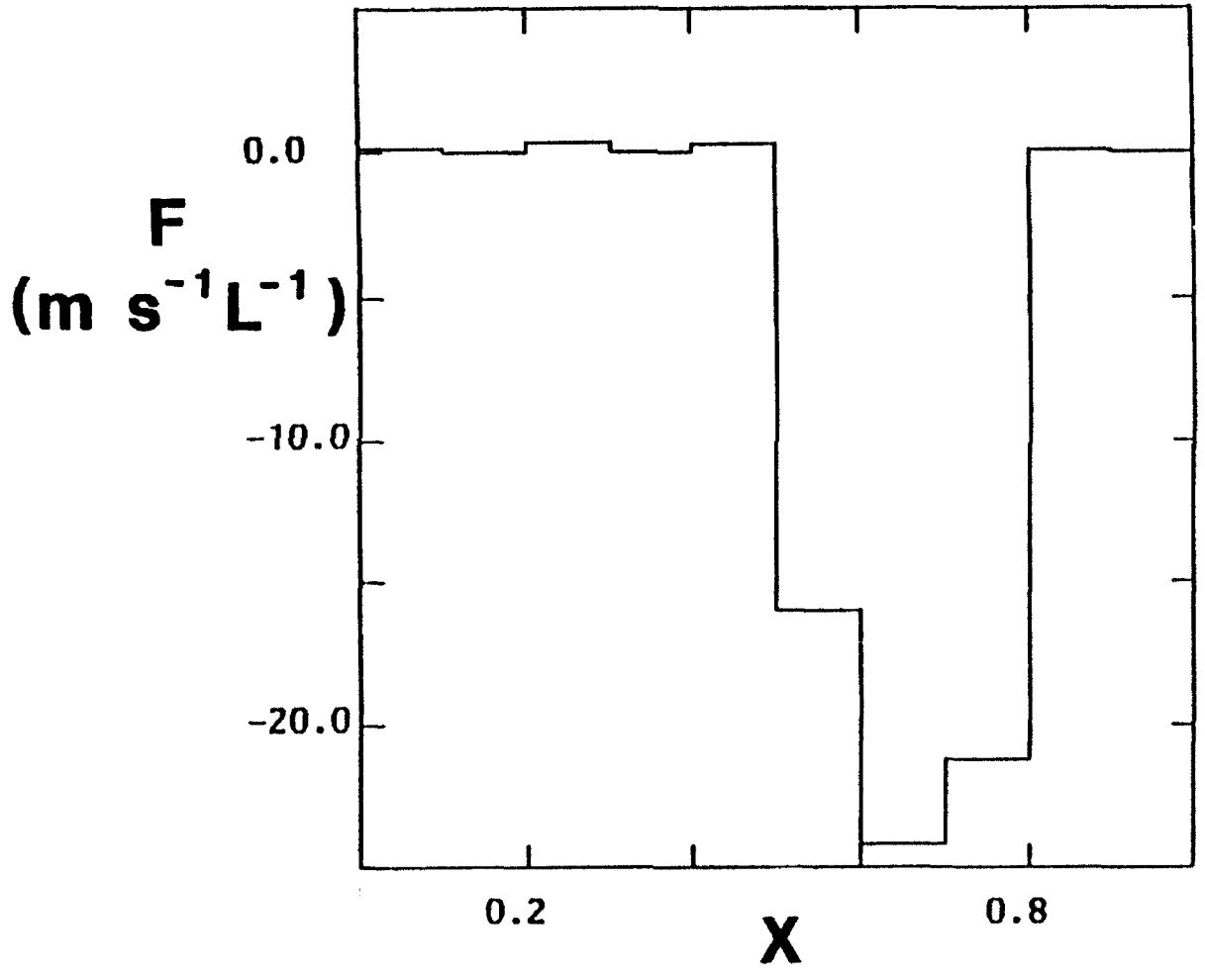
0.0
F
(m s^{-1}L^{-1})
-10.0
-20.0
0.2
0.8
X

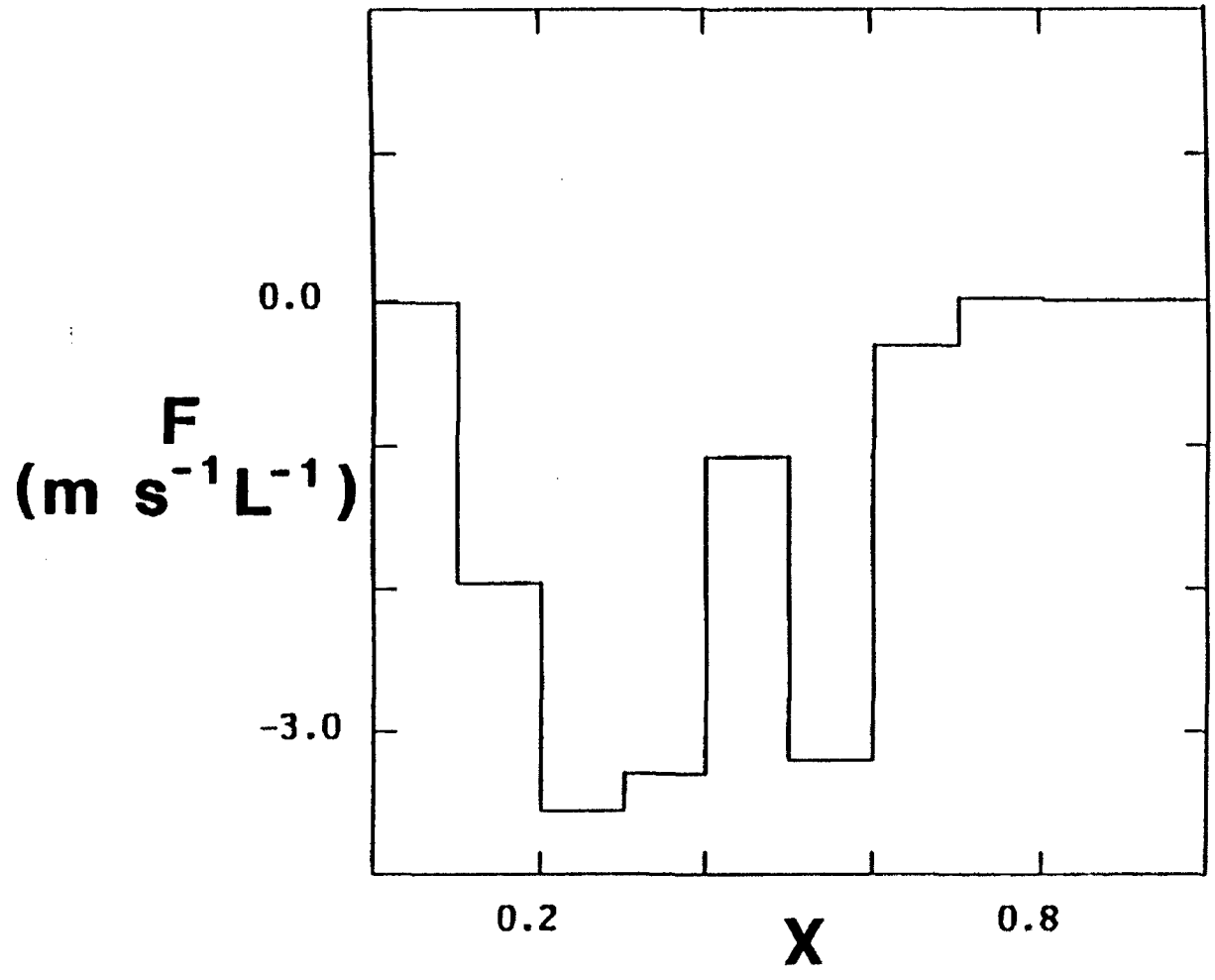
0.0
-3.0
F
(m s^{-1}L^{-1})
0.2
0.8
X

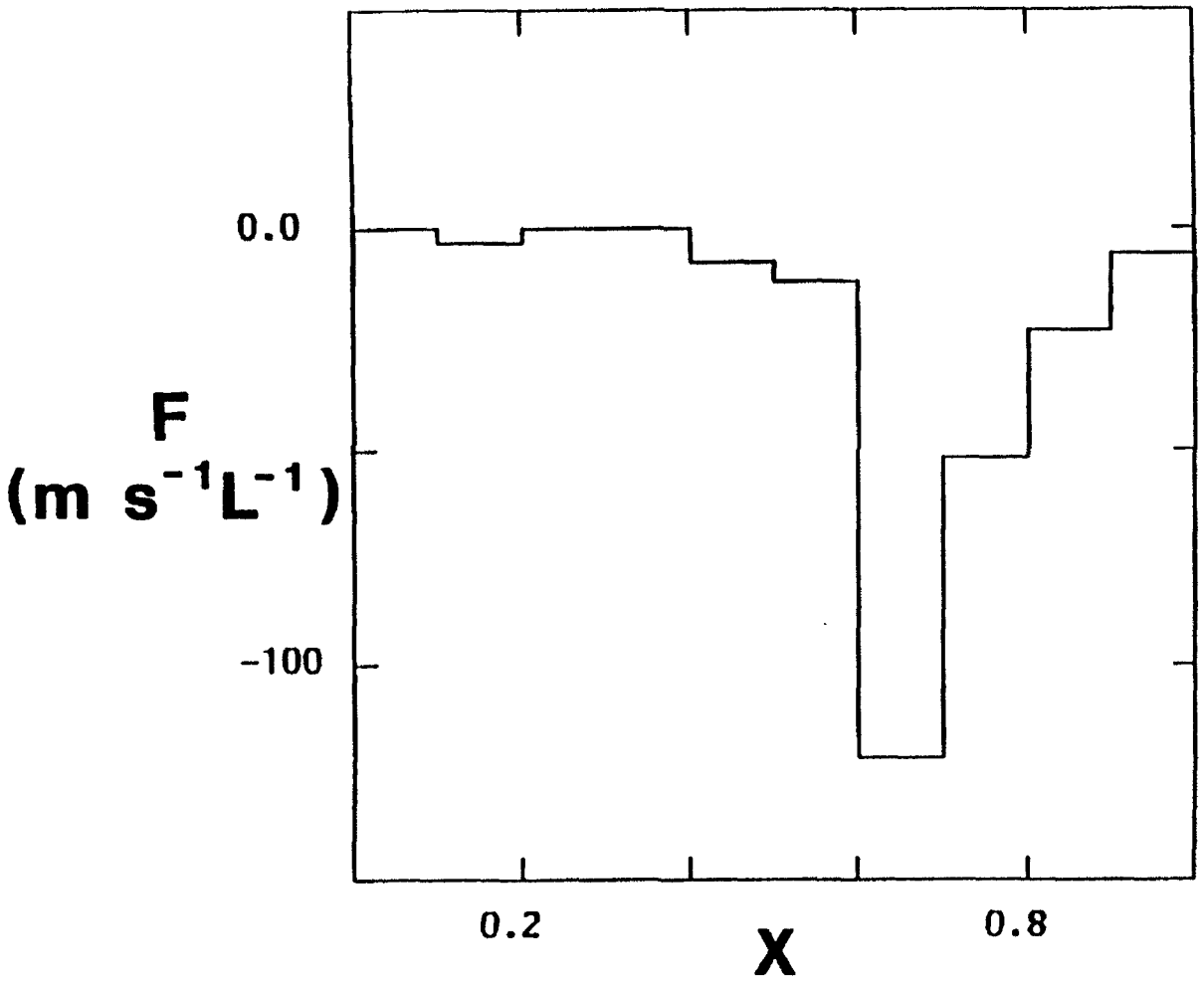
0.0
-100
F
(m s^{-1}L^{-1})
0.2
0.8
X

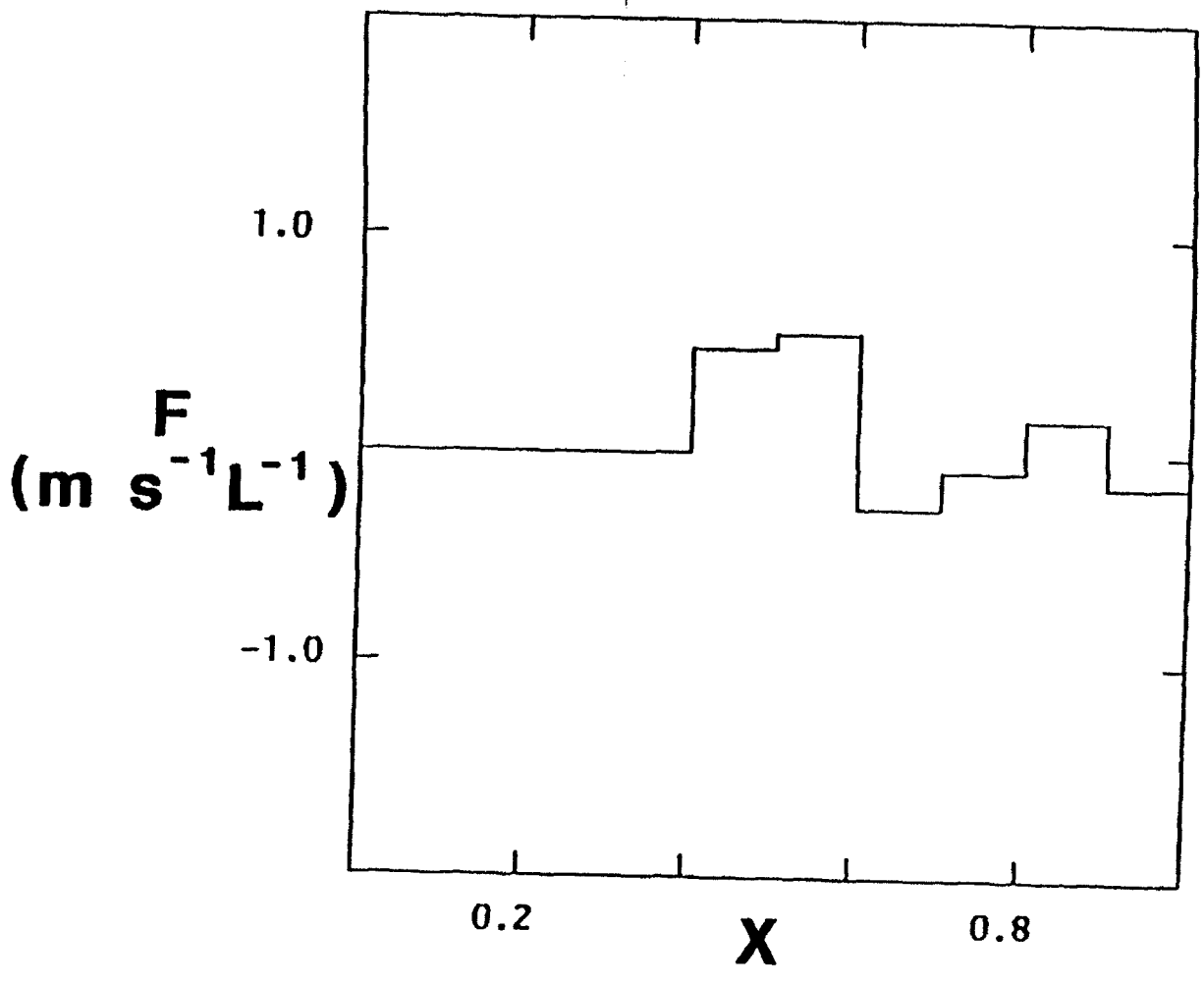
1.0
F
(m s^{-1}L^{-1})
-1.0
0.2
X
0.8

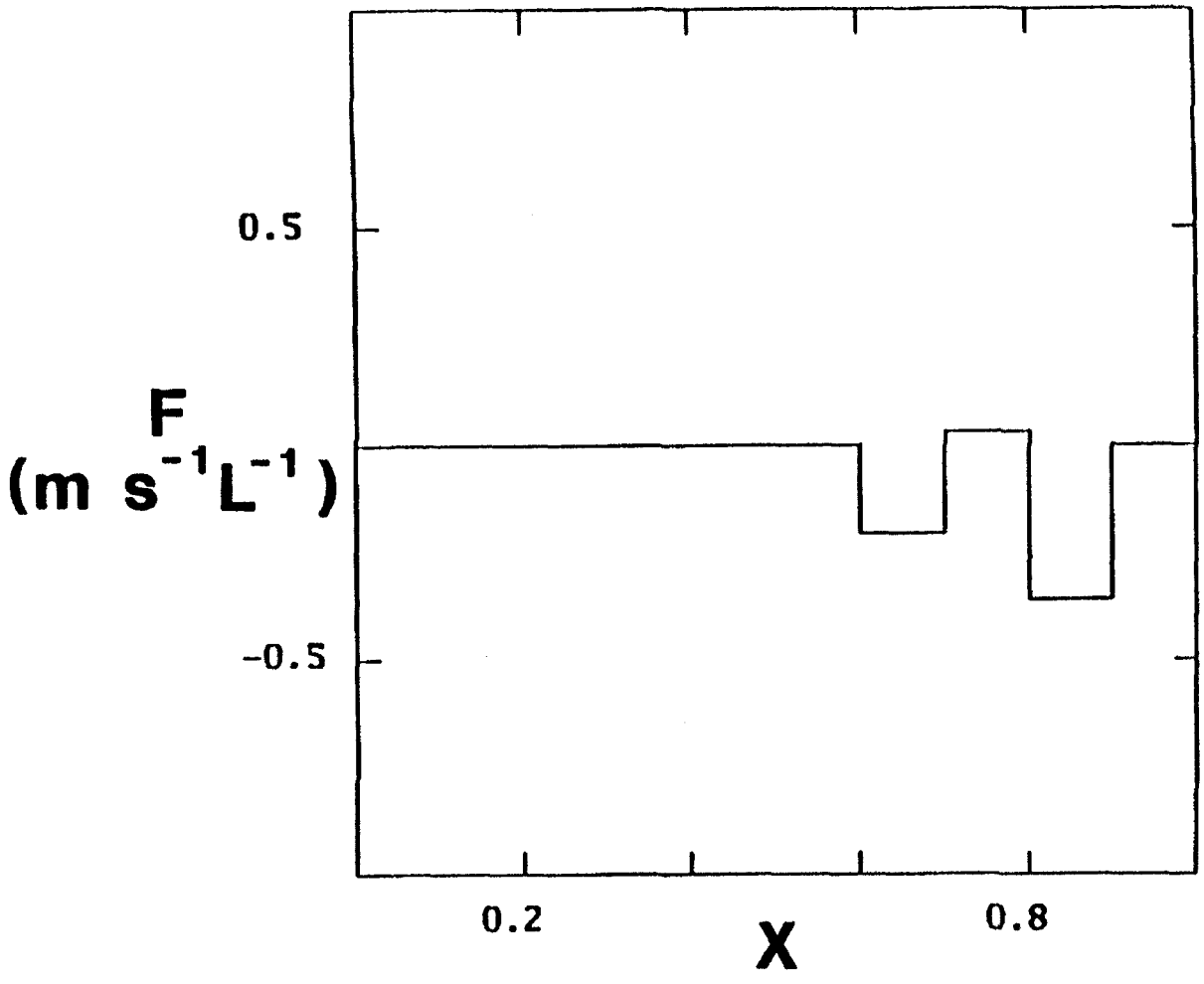
0.5
F
(m s^{-1}L^{-1})
-0.5
0.2
0.8
X

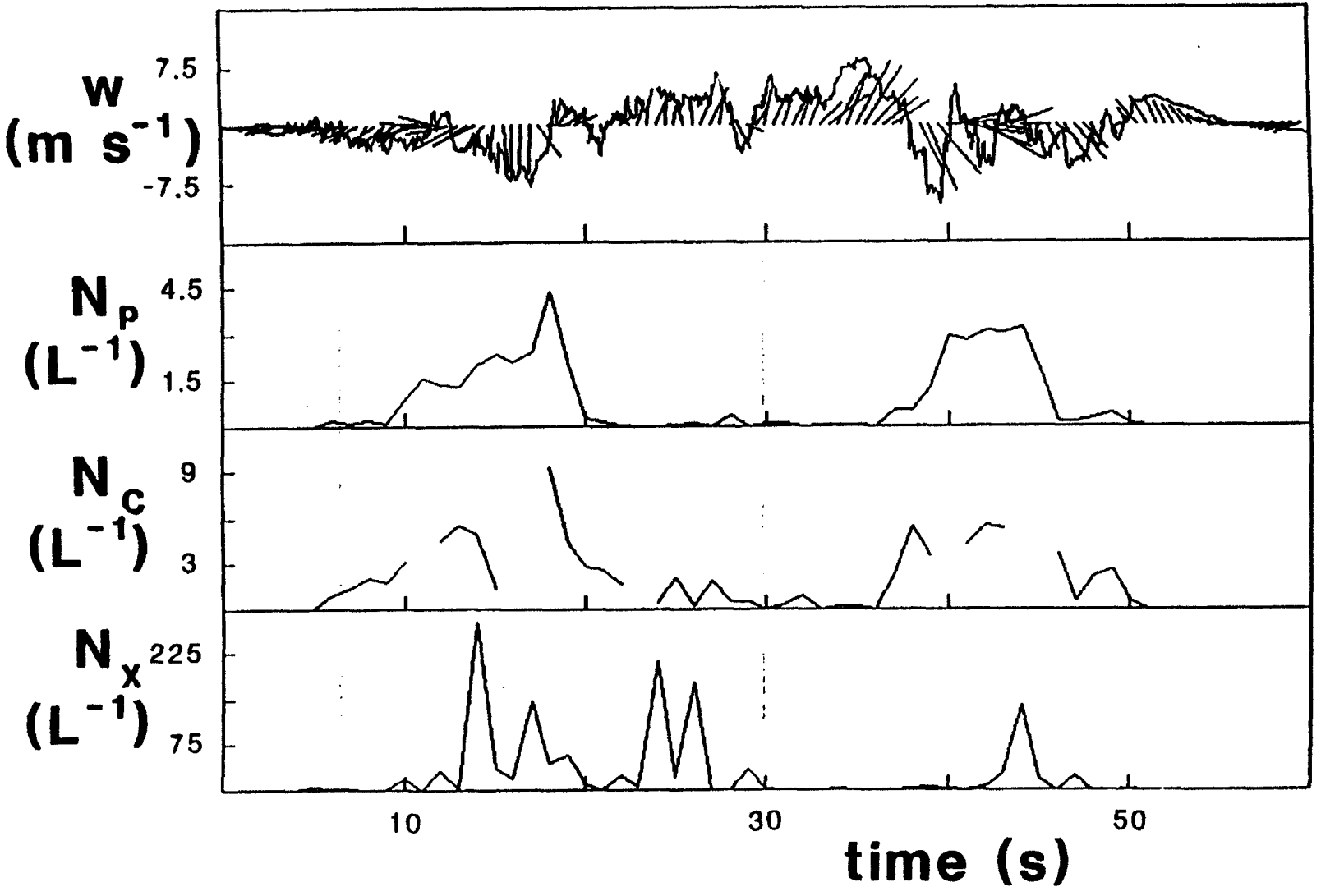
W
(m s^{-1})
7.5
-7.5
N_P
(L^{-1})
4.5
1.5
N_C
(L^{-1})
9
3
N_X
(L^{-1})
225
75
10
30
50
time (s)

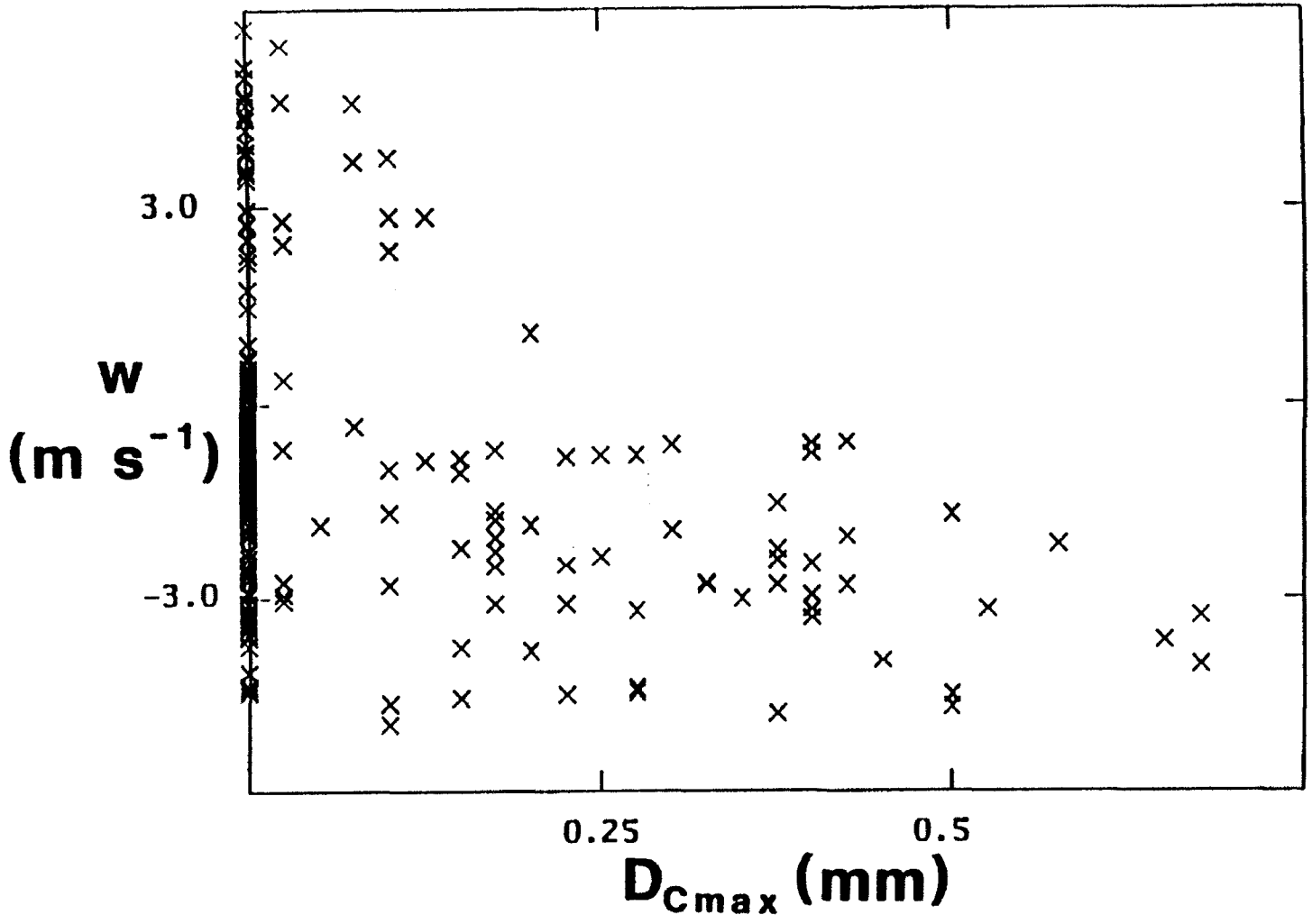
3.0
-3.0
w
(m s^{-1})
0.25
0.5
D_{Cmax} (mm)

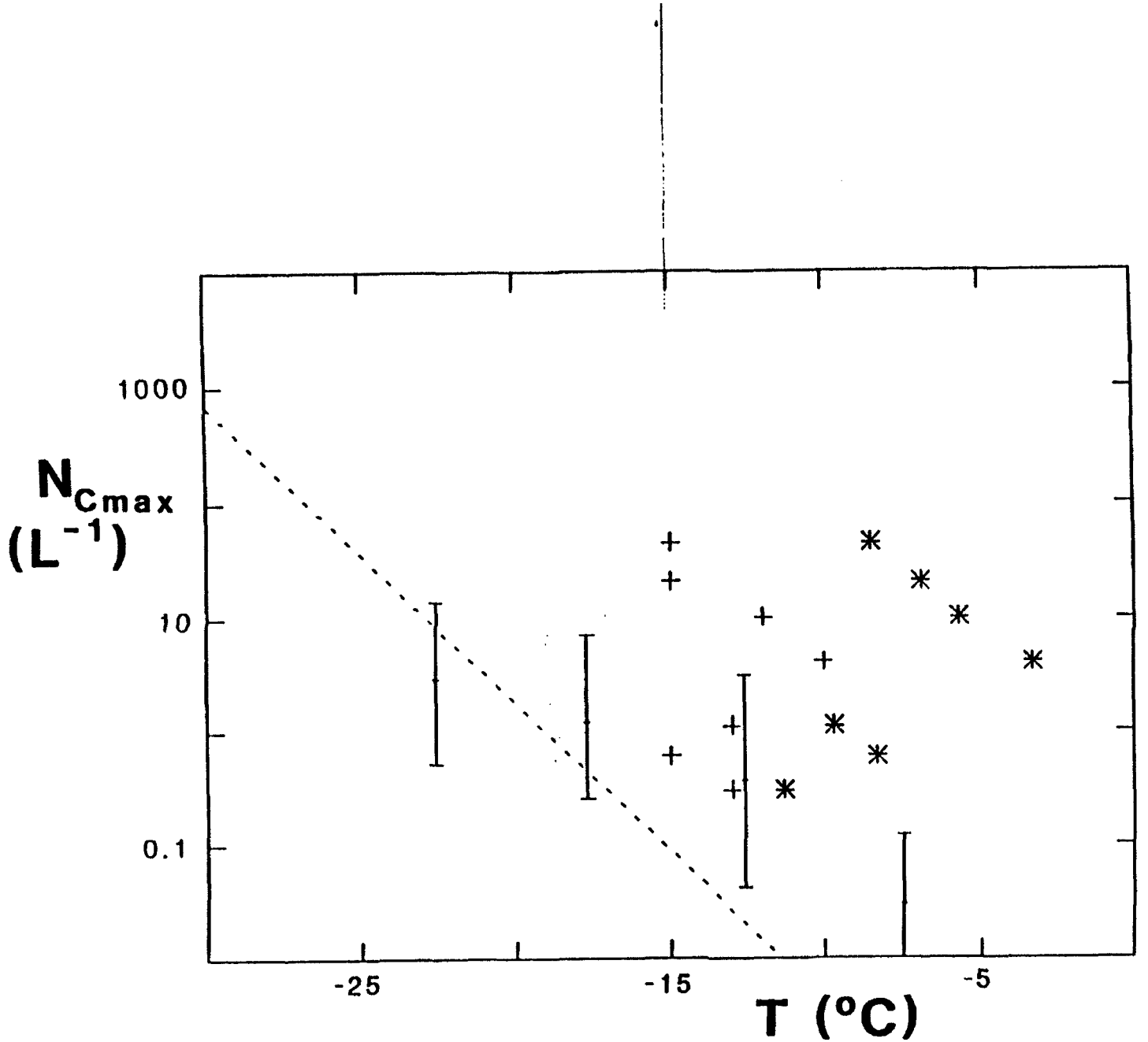
1000
10
0.1
N_{Cmax}
(L^{-1})
-25
-15
-5
T (°C)

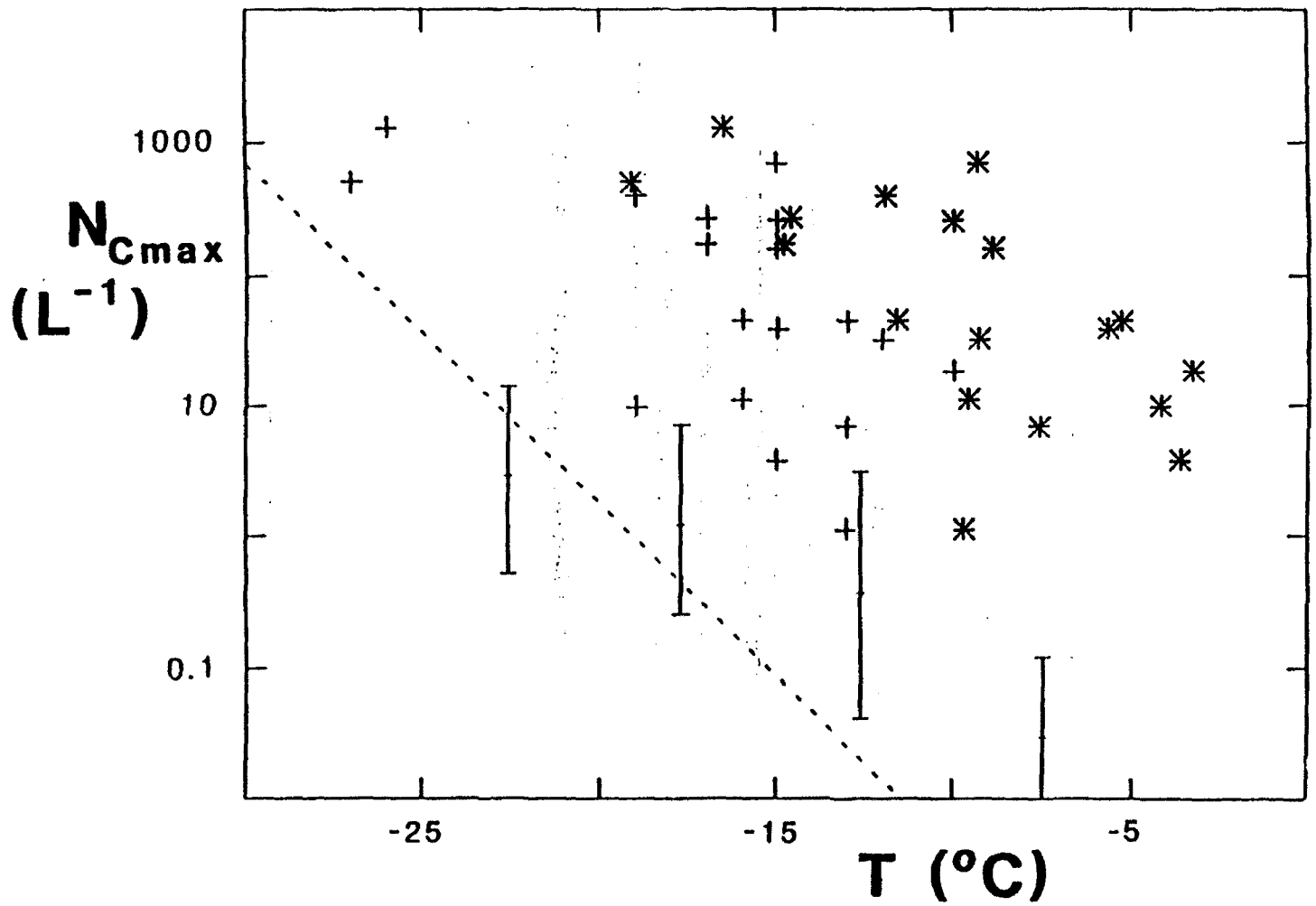
1000
10
0.1
N_{Cmax}
(L^{-1})
-25
-15
-5
T (°C)

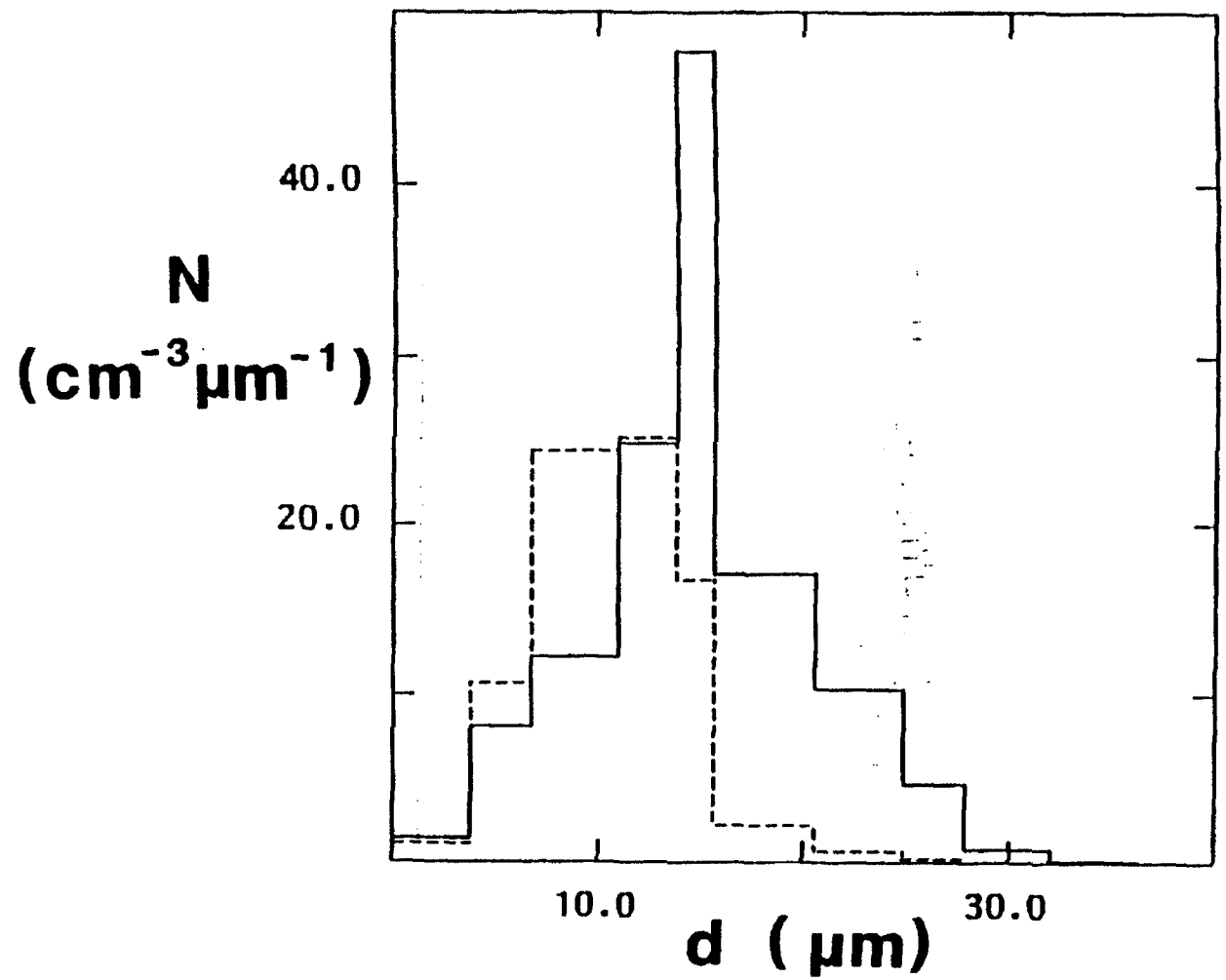
40.0
20.0
N
(cm⁻³μm⁻¹)
10.0
30.0
d (μm)

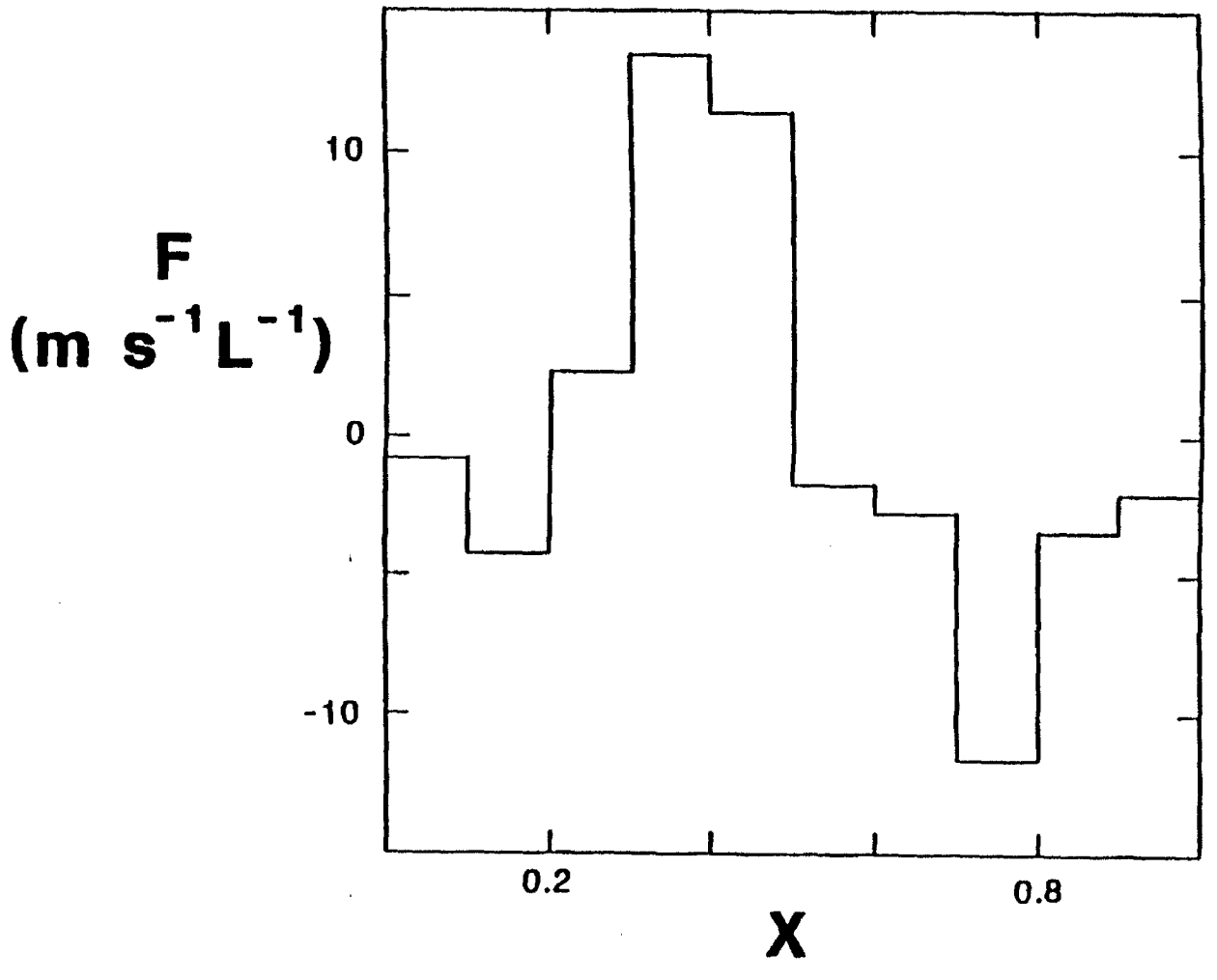
F
(m s^{-1}L^{-1})
10
0
-10
0.2
0.8
X

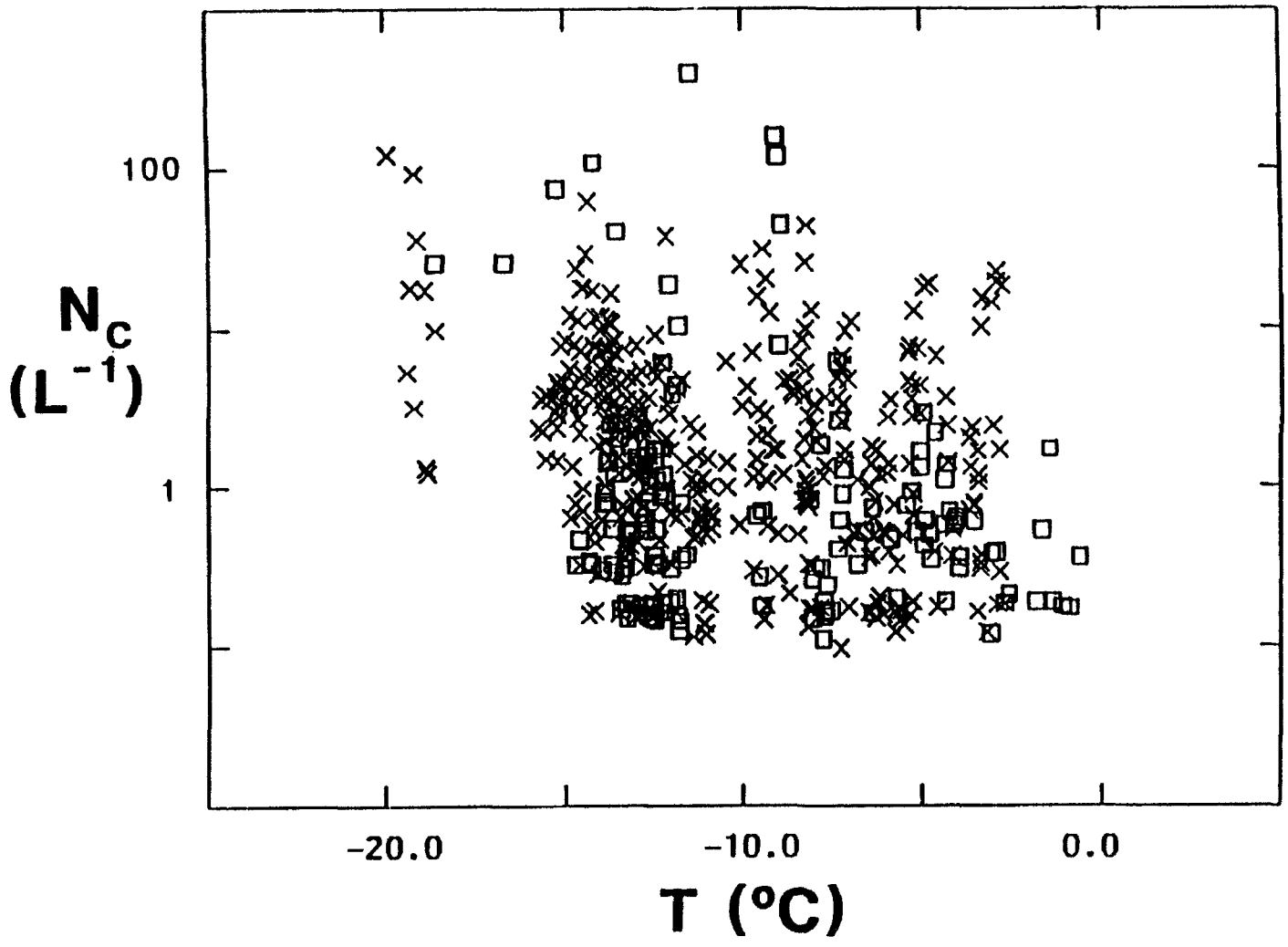
100
1
N_C
(L^{-1})
-20.0
-10.0
0.0
T (°C)

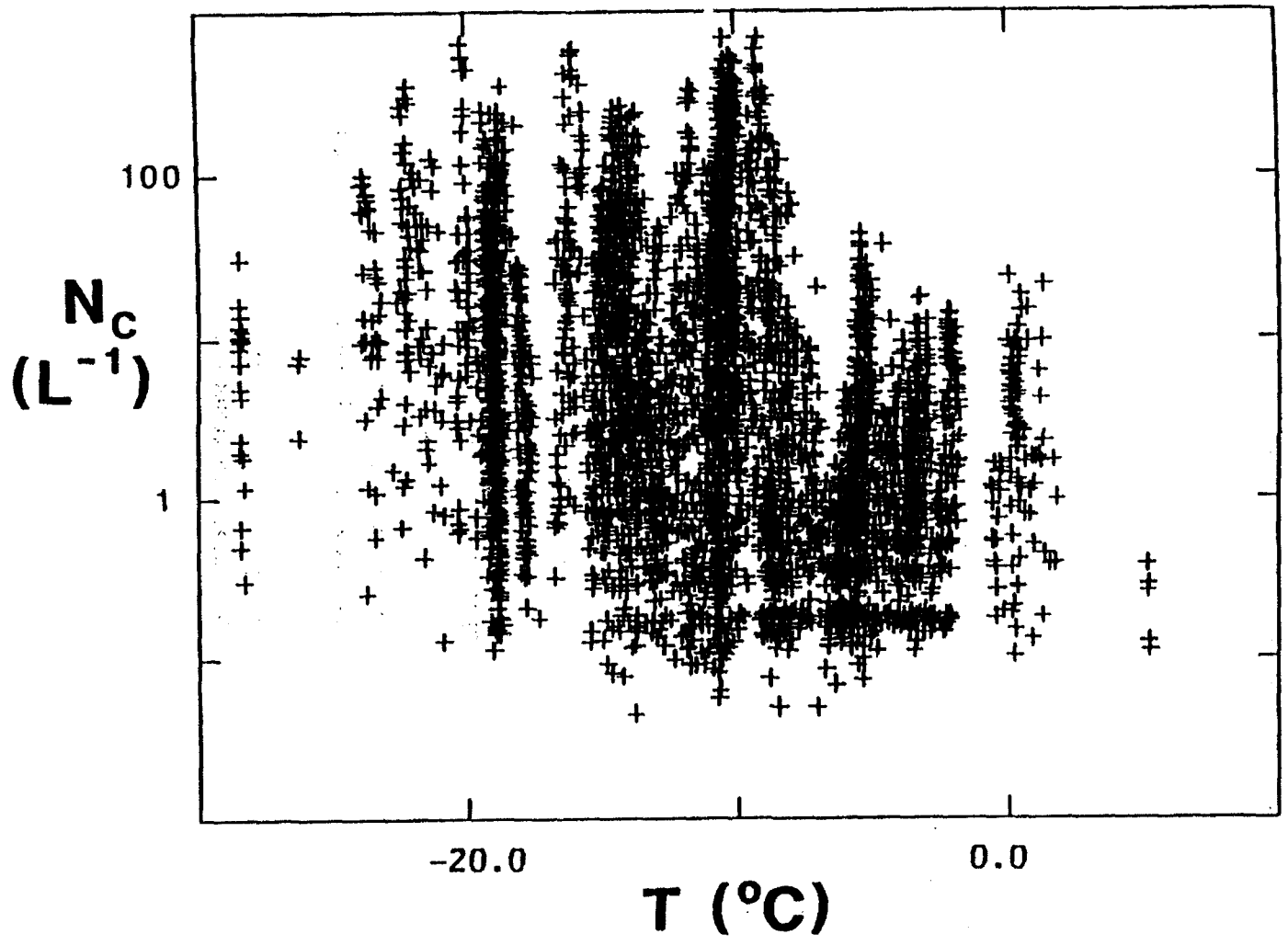
100
1
N_C
(L^{-1})
-20.0
0.0
T (°C)

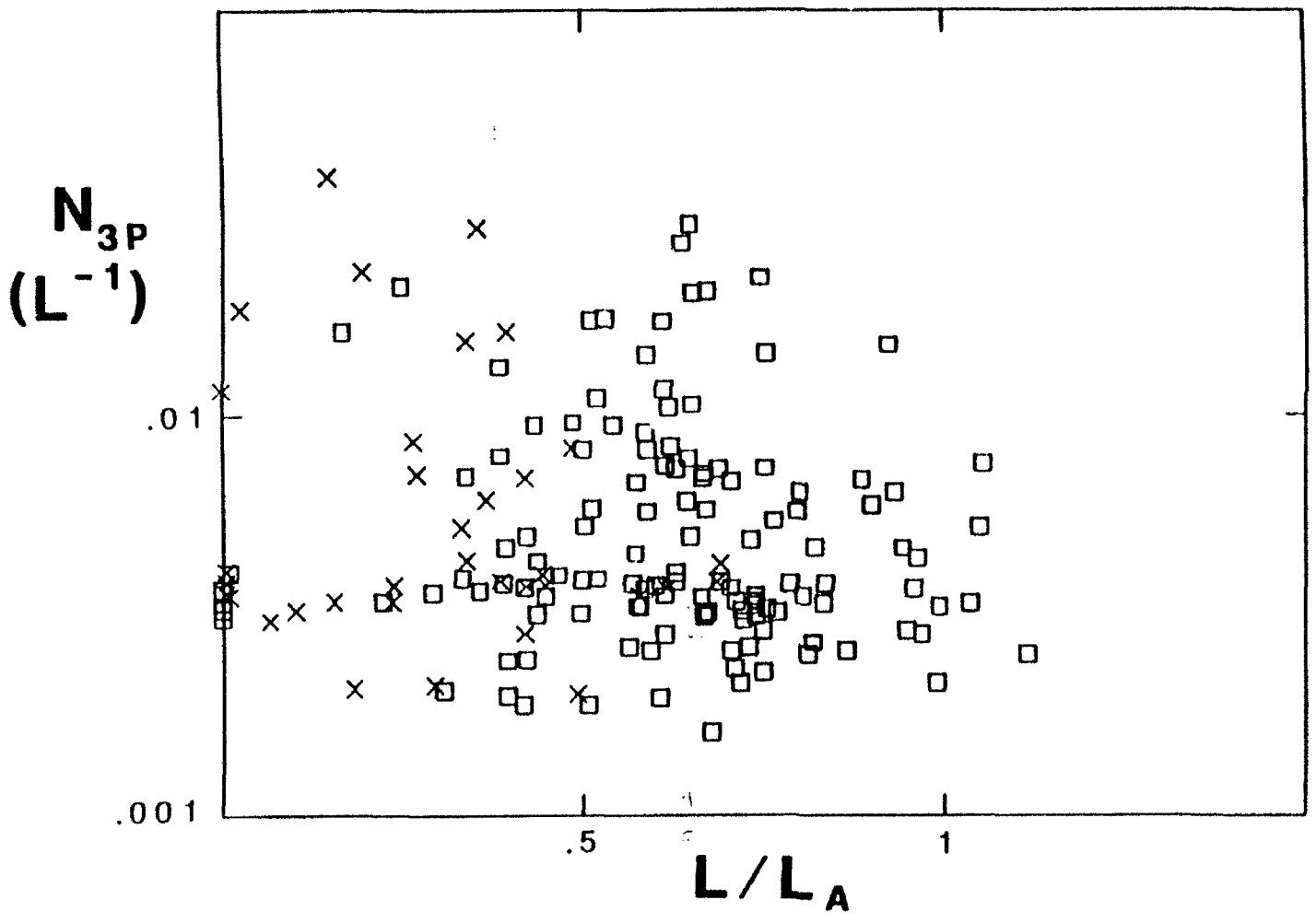
N_{3P}
(L^{-1})
.01
.001
.5
1
L/L_A

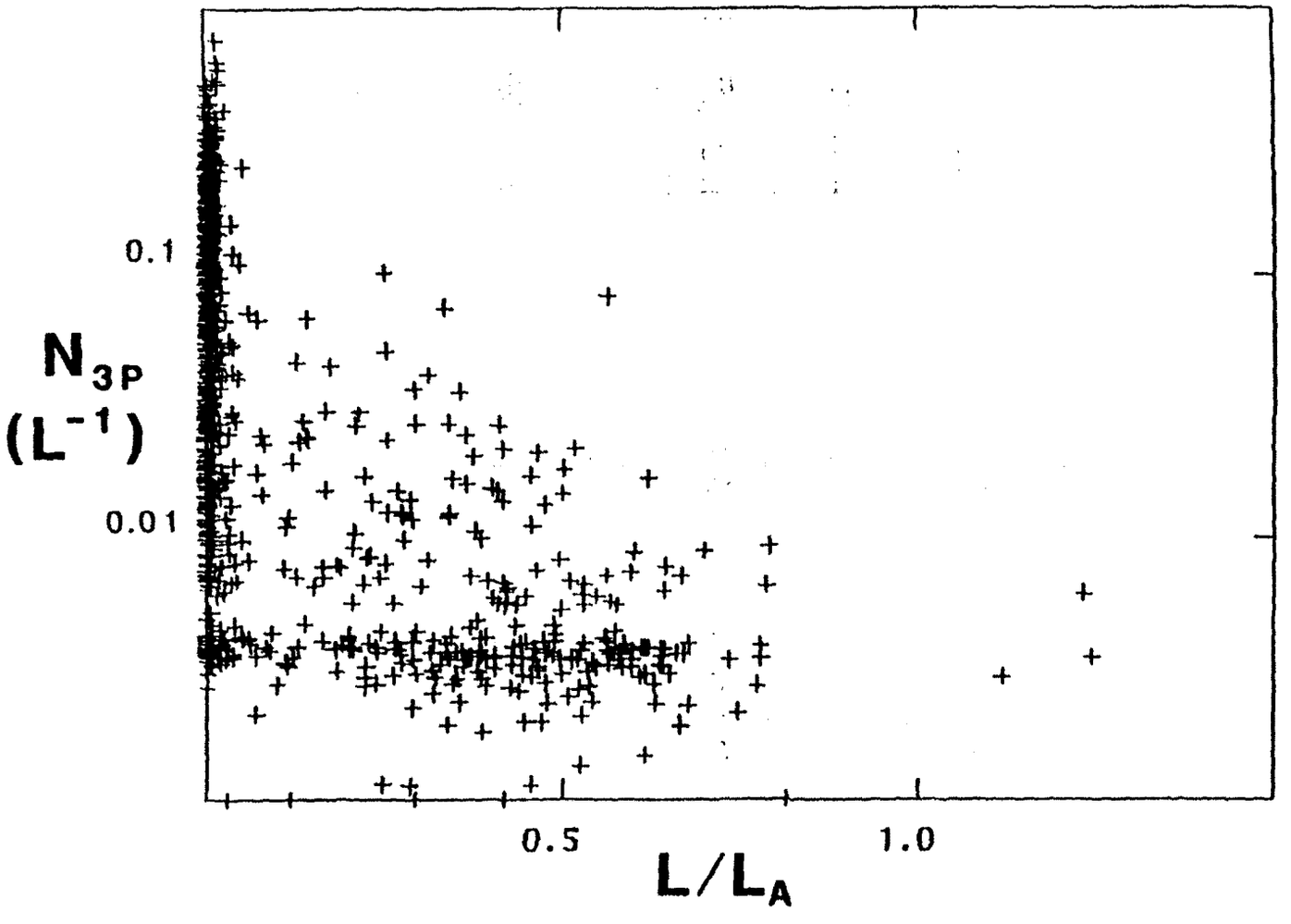
0.1
0.01
N_{3P}
(L^{-1})
0.5
1.0
L/L_A

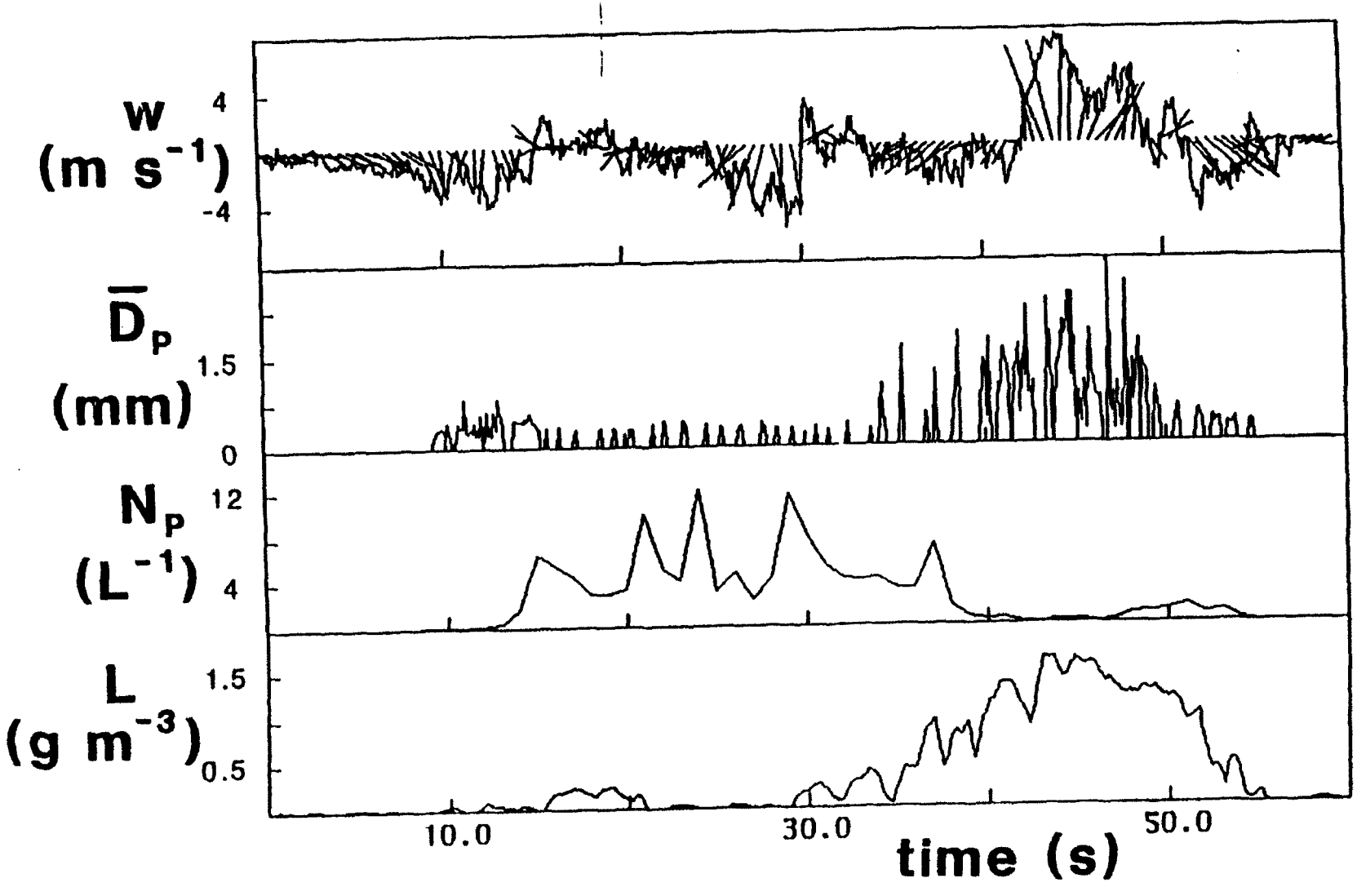
w
(m s^{-1})
4
-4
$\overline{D}_P$
(mm)
1.5
0
N_P
(L^{-1})
12
4
L
(g m^{-3})
1.5
0.5
10.0
30.0
50.0
time (s)

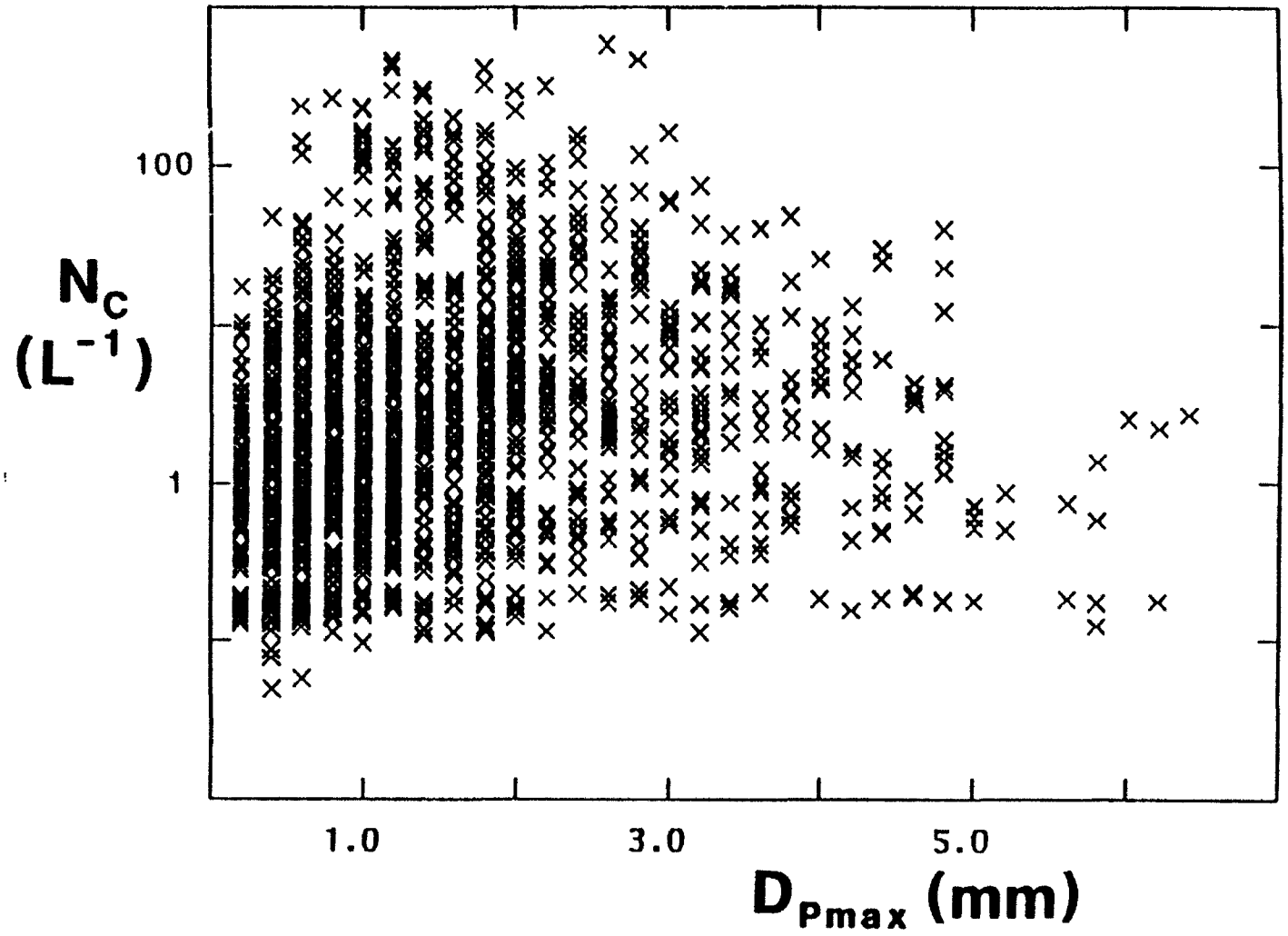
100
1
N_C (L^{-1})
1.0
3.0
5.0
D_{Pmax} (mm)

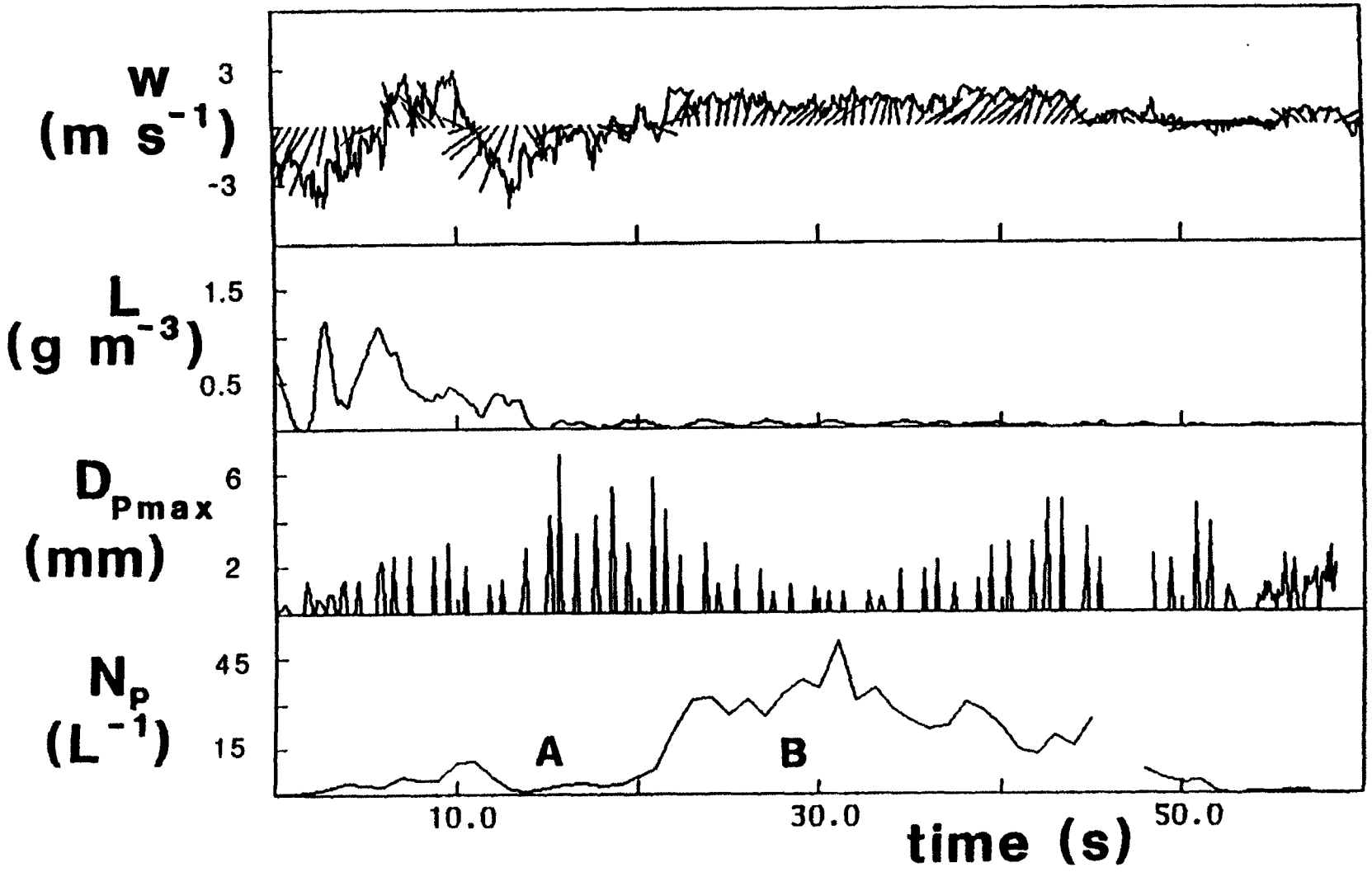
w
(m s^{-1})
3
-3
L
(g m^{-3})
1.5
0.5
D_{Pmax}
(mm)
6
2
N_P
(L^{-1})
45
15
A
B
10.0
30.0
50.0
time (s)

A

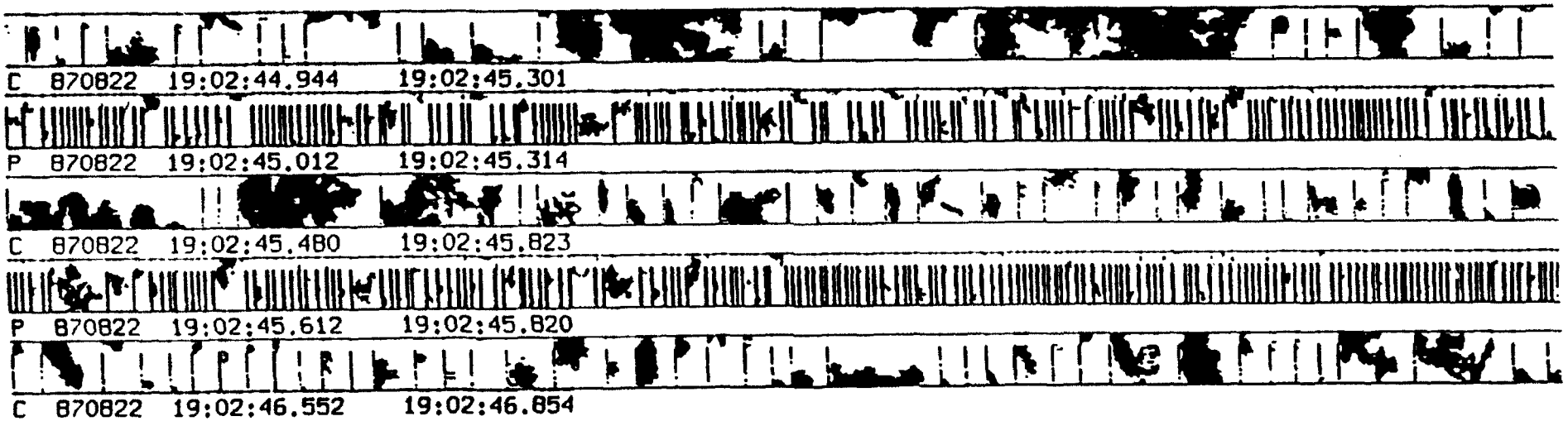
C 870822 19:02:44.944 19:02:45.301
P 870822 19:02:45.012 19:02:45.314
C 870822 19:02:45.480 19:02:45.823
P 870822 19:02:45.612 19:02:45.820
C 870822 19:02:46.552 19:02:46.854

B

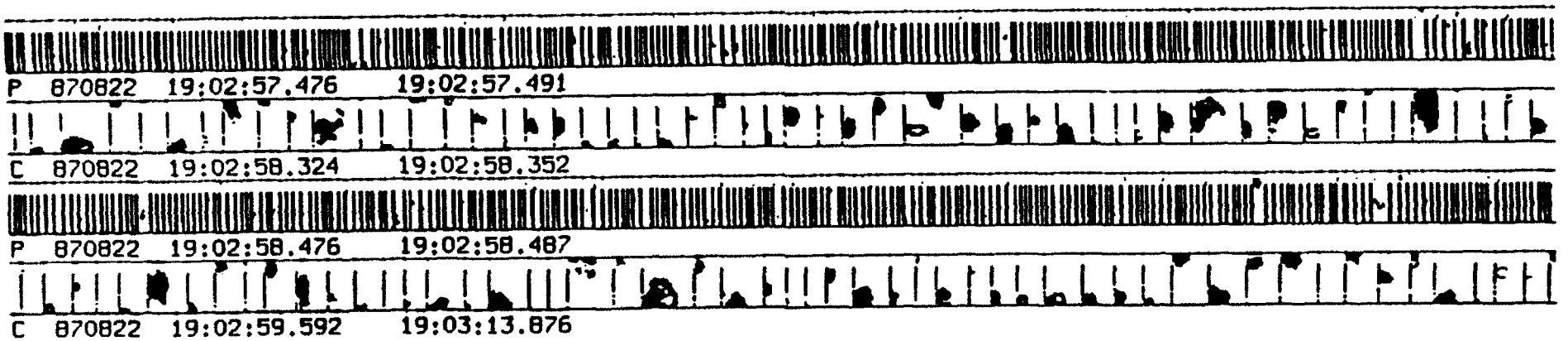
P 870822 19:02:57.476 19:02:57.491
C 870822 19:02:58.324 19:02:58.352
P 870822 19:02:58.476 19:02:58.487
C 870822 19:02:59.592 19:03:13.876

Proceedings of the Ninth International Conference in Atmospheric Electricity, St. Petersburg, Russia, 1992)

CORONA INITIATION IN THUNDERCLOUDS

A.M.Blyth (1), H.J.Christian (2) and J. Latham (3).

(1) Physics Dept, NMIMT, Socorro, New Mexico 87801, USA
(2) NASA/MSFC, Huntsville, Alabama 35812, USA
(3) Physics Dept, UMIST, PO BOX 88, Manchester M60 1QD, UK

Macroscopic electric fields in excess of about 400kV/m probably do not exist in thunderclouds (1). The only two mechanisms which appear capable, in such fields, of producing corona - initiatory to lightning - involve protuberances on hydrometeors of precipitation dimensions; individual ice particles (2), or pairs of colliding warm raindrops (3).

Thus the threshold field Ec for corona emission depends upon the characteristics of the hydrometeors, and breakdown will not necessarily occur in a thundercloud in the region of highest field: which has hitherto been assumed in modelling studies.

The objectives of our laboratory work were to: (a) extend the range of conditions over which Ec values are known for colliding raindrops; (b) perform similar experiments for supercooled raindrops; (c) measure Ec values associated with the collisions of supercooled drops with ice particles. In addition, data from airborne studies of thunderstorms in New Mexico were examined to establish the salient hydrometeor characteristics in regions of strong field. Figures (1) and (2) illustrate the presence of both supercooled raindrops and ice particles large enough to produce corona in fields below about 400kV/m.

The laboratory experiments (a) and (b) involved the same apparatus and procedures as described in (3). The experiments (c) utilised basically the same set-up as that described in (2), with the addition that drops fell through a hole in the upper electrode and collided with artificially produced snowflakes or hailstones mechanically suspended in a vertical electric field. The velocities of impact V in these experiments were consistent with those that obtain in thunderstorms.

Figures 3,4 and 5 present data obtained in experiments (a), (b) and (c) respectively. In each case, histograms are plotted of the measured probability F of corona emission as a function of the electric field E. It is seen that for all three types of interaction a significant probability exists of corona initiation in fields below 400kV/m. Photographs showed that glancing collisions produced ephemeral liquid filaments generally longer than the hydrometeor dimensions, drawn out at a shallow angle to E. Since the electrical relaxation time is substantially less tha the lifetime of these conducting filaments (around 1ms) the observed corona was almost certainly emitted from their tips.

Figure 6 shows that for a constant impact parameter, the threshold field Ec for a 50% probability of corona emission was lowest at an intermediate value of impact velocity V.

Acknowledgements This work was supported by USAFOARD and NSF.

References.

1. R.F. Griffiths and J. Latham, 1974, QJRMS, 100, 163-180.
2. J.A. Crabb and J. Latham, 1974, QJRMS, 100, 191-202.
3. J. Latham, 1981, QJRMS, 107, 277-298.

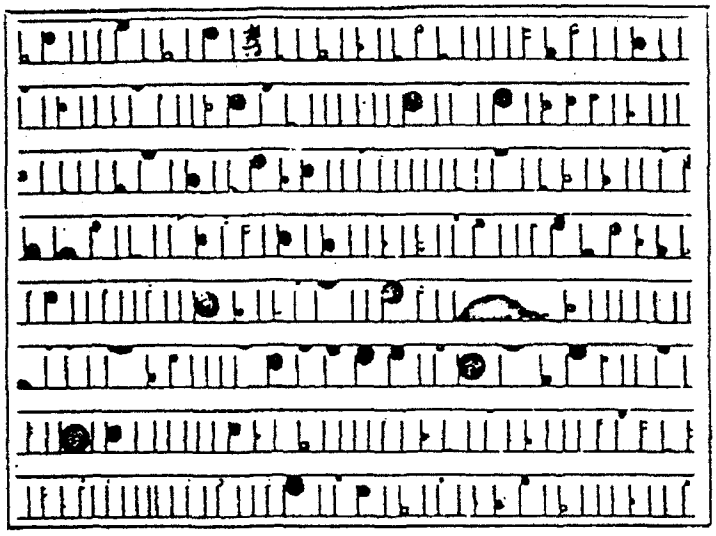

Figure 1 (1 = 0.8 mm)

Figure 2 (1 = 0.8 mm)

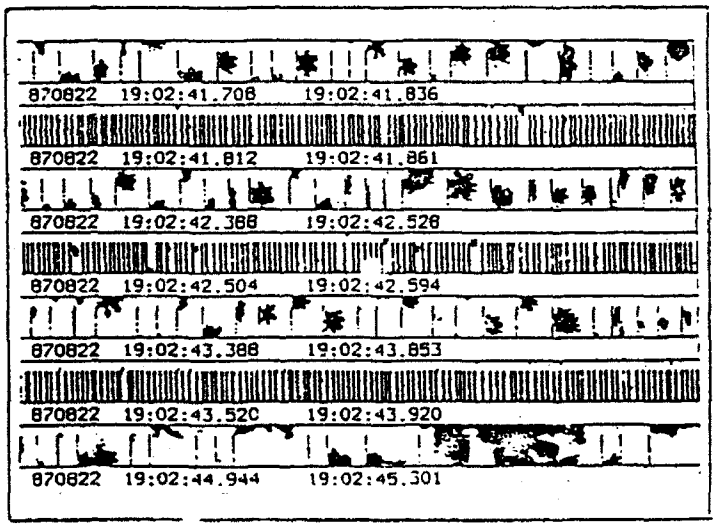

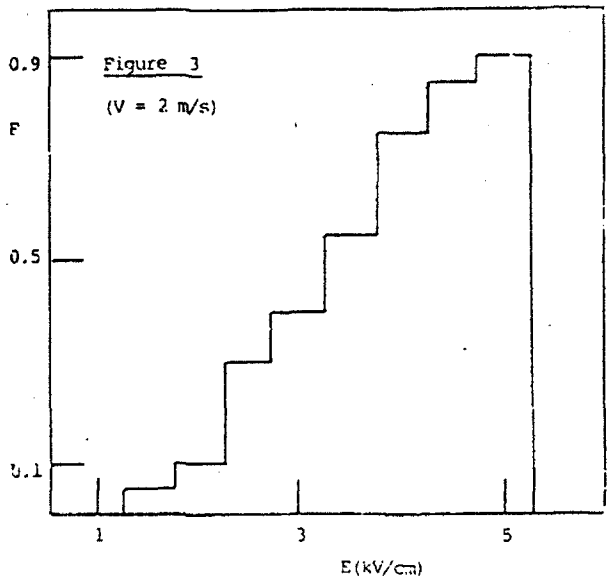

Figure 3
(V = 2 m/s)

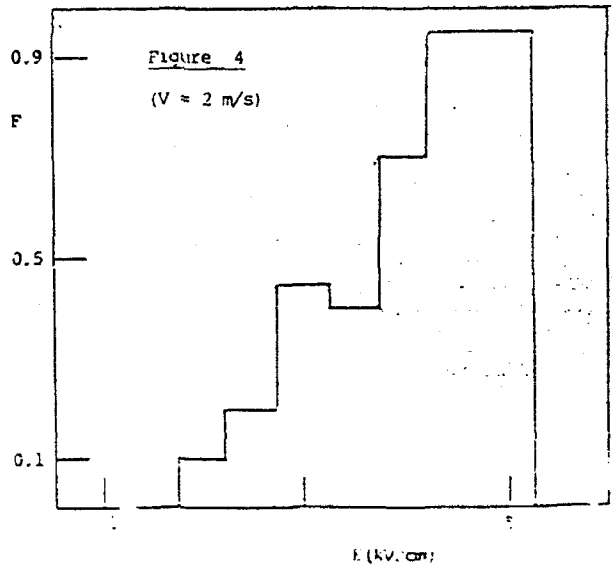

Figure 4
(V = 2 m/s)

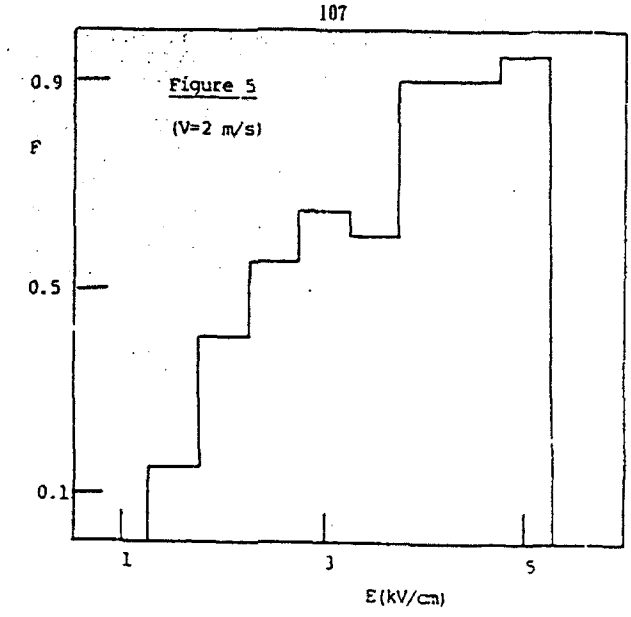

Figure 5

(V=2 m/s)

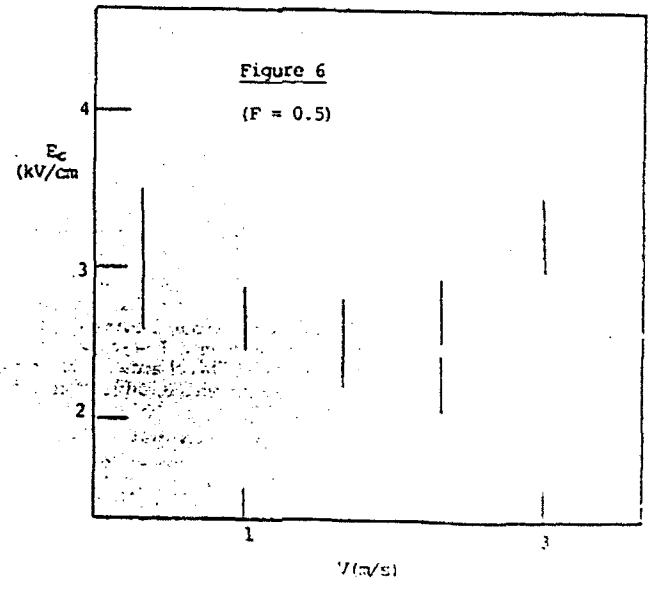

Figure 6

(F = 0.5)